The development of novel microneedle arrays fabricated from hyaluronic acid, and their application in the transdermal delivery of diabetes drugs

Shu LIU

Department of Biopharmaceutics,

Kyoto Pharmaceutical University

2014

TABLE OF CONTENTS

ABBREVIATIONS

AAC	Area above the curve
AUC	Area under the curve
ELISA	Enzyme-linked immunosorbent assay
FD4	Fluorescein isothiocyanate-labeled dextran with an average molecular weight of 4kDa
H&E	Hematoxylin and eosin
HA	Hyaluronic acid
HPLC	High performance liquid chromatography
IPGTTs	Intraperitoneal glucose tolerance tests
MNs	Microneedle arrays
O.C.T	Optimal cutting temperature
P.I.I.	Primary irritation index
PBS	Phosphate-buffered saline
PET	Polyethylene terephthalate
SEM	Scanning electron micrographs
STZ	Streptozotocin
TER	Transcutaneous electrical resistance
TEWL	Transepidermis water loss
TFA	Trifluoroacetic acid

ABSTRACT

Traditional non-invasive transdermal patch systems are simple and comfortable to use, but the choice of therapeutics is limited to small molecules due to the existence of stratum corneum. To overcome this skin barrier, microneedle arrays (MNs) have gained increasing attention as a novel minimally invasive method and they are able to deliver a variety of molecules into the skin, including small drugs, macromolecules, nanoparticles and fluid extracts. MNs have been demonstrated to effectively penetrate the stratum corneum into the epidermis and/or superficial dermis to administer compounds into the skin for local or systemic administration. Their sharp tips and target insertion depth reduce the risk of encountering the nerves that perceive pain. Among numerous research works regarding MNs, the ones made of biocompatible and biodegradable polymers and carbohydrates appear to be an attractive drug delivery system. They have the potential for loading drugs into a matrix of needles and efficiently releasing them in the skin by biodegradation or dissolution in the interstitial fluid; a one-step application. If left in the skin, these types of needles safely degrade and eventually disappear, which are free from the risk of complications of the ones fabricated from silicon, metal and glass.

Based on these observations, in this study, novel dissolving MNs fabricated from hyaluronic acid (HA) were developed, evaluated their characteristics and assessed the improvement on transdermal delivery of relatively high molecular weight drugs. Moreover, insulin-loaded MNs with insulin containing in whole needles were fabricated and characterized their ability of transdermal delivery of insulin to type 1diabetic rats in an *in vivo* system. Furthermore, in order to minimize the wastage of drug, accurately control the drug dose and achieve a fast drug delivery, exendin-4 tip-loaded MNs were developed and investigated their acute efficacy in type 2 diabetic GK/Slc rats in an *in vivo* system.

1. The characteristics of novel microneedle arrays fabricated from hyaluronic acid

MNs fabricated from HA have 190 microneedles in a circular array with a diameter of 10 mm. Each needle was approximately 800 μm in height, and had a diameter of 160 μm at the base and 40 μm at the tip. After being inserted into the dermis, they created drug permeation pathways that had a similar shape to the inserted MNs in the histological cross-section of skin. The MNs containing blue dyes uniformly created pathways on surface of rat skin, and the blue dots corresponded to the injection sites of the MNs. After the application onto rat skin *in vivo*, MNs appeared to slightly dissolve at 5 min and approximately completely dissolve within 1 h. Moreover, the MNs significantly increased transepidermal water loss and reduced transcutaneous electrical resistance, indicating that they could puncture the skin and create drug permeation pathways successfully. Both of the value almost recovered to baseline levels in the MN group, and relatively small pathways created by the microneedles rapidly recovered as compared with those created by a tape stripping treatment. Slight erythema but no edema appeared at the injection sites at 1 h and disappeared within 24 h. The primary irritation index of the MNs was calculated to be 1.7, indicating that irritation and skin damage caused by MNs were slight. Furthermore, in this study, fluorescein isothiocyanate-labeled dextran with an average molecular weight of 4 kDa (FD4) was used as a model drug with a relatively high molecular weight. It was found that the transdermal permeability of FD4 using the MNs was much higher than that of the FD4 solution. Furthermore, the MNs were much more effective for increasing the amount of FD4 accumulated in the skin. These findings indicated that using novel MNs fabricated from HA is a very useful and effective strategy to improve the transdermal delivery of drugs, especially relatively high molecular weight drugs without seriously damaging the skin.

2. Application in the transdermal delivery of diabetes drugs

Insulin-loaded MNs with insulin containing in whole needles were uniform in size with

sharp tips. They maintained their skin piercing abilities for at least 1 h, even at a relative humidity of 75 %. After storing insulin-loaded MNs for a month at −40, 4, 20, and 40 °C, more than 90 % of insulin remained in MNs at all temperatures. It was also found that insulin was released from MNs at a relatively constant rate via an *in vitro* release study, and the majority of the insulin was released within 1 h. These findings were consistent with the complete dissolution of MNs within 1 h of application to rat skin *in vivo*. Therefore, the novel HA MNs possess self-dissolving properties after their dermal application, and insulin appears to be rapidly released from these MNs. Furthermore, a dose-dependent hypoglycemic effect and transdermal delivery of insulin were observed after a dermal treatment with insulin-loaded MNs *in vivo*. A continuous hypoglycemic effect was observed after 0.25 IU of insulin was administered to skin via MNs. Additionally, lower peak plasma glucose levels, but higher plasma insulin concentrations after 2 h, were achieved with 0.25 IU of insulin administered via MNs as compared to the subcutaneous administration of insulin of the same dose. Pharmacodynamic and pharmacokinetic parameters indicated that insulin administered via MNs was almost completely absorbed from the skin into the systemic circulation, and that the hypoglycemic effect of insulin-loaded MNs was almost similar to that of the subcutaneous injection of insulin. These findings indicate that the novel insulin-loaded MNs fabricated from HA are a very useful alternative method of delivering insulin via the skin into the systemic circulation without inducing serious skin damage.

In order to further improve the efficacy of soluble MNs, drug tip-loaded MNs were designed and developed. FD4 was selected as a model drug, and content in FD4 tip-loaded MNs was shown with standard error below 10 % in the microneedles with dosage of 1, 2 and 4 μg/patch. *In vitro* release of drug was rapid even at 30 s at the beginning, and the majority of the FD4 was released within 5 min. Furthermore, in the acute efficacy study in type 2 diabetic GK/Slc rats, exendin-4 tip-loaded MNs showed a nearly equivalent efficacy as subcutaneous injection on glucose tolerance and enhancement of insulin secretion. The

pharmacokinetic property of exendin-4 tip loaded MNs was observed closely matched the same dosage exendin-4 subcutaneous injection.

In conclusion, these findings indicate that the novel soluble MNs fabricated with HA were very useful alternative method to deliver drug from the skin to the systemic circulation without serious skin damage. Therefore, the HA MNs might be effective and safe dosage form for transdermal delivery of insulin and exendin-4 in clinical applications for the treatment of diabetes.

INTRODUCTION

Traditional non-invasive transdermal patch systems are simple and comfortable to use, but the choice of therapeutics is limited to small molecules due to the existence of stratum corneum. To overcome this skin barrier, MNs have gained increasing attention as a novel minimally invasive method [1, 2]. Needles with micrometer dimensions have been demonstrated to effectively penetrate the skin barrier of the stratum corneum and create efficient pathways for the delivery of small drugs, macromolecules and nanoparticles, as well as for fluid extraction [3-6]. They are long enough to penetrate the stratum corneum and provide precise penetration depth under the skin by controlling the length of the needles [7]. Their sharp tips are short enough to reduce damage to skin nerves and pain [8, 9], and narrow enough to induce minimal trauma and reduce the opportunities for infections to develop during insertion [10]. Therefore, this novel approach was proposed as a hybrid to combines the advantages of conventional injection needles and transdermal patch while minimizing their disadvantages.

In previous researches, most microneedles have been fabricated from silicon [11-13], metal [14-16] and glass [17]. Since the loading amounts of drugs into these types of microneedles are quite limited, these needles have been used for the skin treatment before or after the application of a topical formulation or patch to facilitate the transdermal absorption of drugs [12, 13, 15].Furthermore, due to the decrease in pore size over time after removal of the needles, only small amounts of drugs can be delivered through the pathways created. In such cases, large amounts of drugs with high concentrations have to be used in order to obtain a detectable effect [18, 19]. Moreover, this two-step application process is cumbersome for patients and prone to errors. To overcome these shortcomings and limitations, microneedles with drug-coated shaft surfaces have been developed recently [11, 20-22]. Model drugs were uniformly coated on needle shafts, and coatings were rapidly dissolved in the skin without

wiping off on the skin surface [21, 22]. However, these microneedles have been limited to small drug doses (micrograms) due to their inherently small volume and surface area. Moreover, there is a critical risk that microneedles can be accidentally broken and remain in the skin for a long period of time, similar to the cases of traditional microneedles fabricated from silicon, metal and glass.

Among numerous research works regarding MNs, attention has been paid to the use of microneedles fabricated from biocompatible and biodegradable polymers [23-25] and carbohydrates [26-30], which are free from the risk of complications. If left in the skin, these types of needles safely degrade and eventually disappear. They also have the potential for loading drugs into a matrix of needles and releasing them in the skin by biodegradation or dissolution in the interstitial fluid; a one-step application. However, during the fabrication of MNs consisting of biodegradable polymers or maltose [23, 28, 31-34], a heating step is required, which may cause the breakdown of heat-sensitive drugs, such as insulin, and in turn, eradicate their pharmacological activities. Additionally, most of the previous polymer needles have slow-degrading characteristics which can retain drugs in the skin for a long period of time. Therefore, they are suitable for sustained delivery of drugs. Unlike polymeric needles, maltose and galactose MNs are readily soluble and dissolve in skin within minutes. However, in a wet environment exceeding humidity levels of 43 % to 50 %, these MNs are rapidly dissolved due to hydrolysis, which leads to a rapid deformation or disappearance of needles, and poor insertion ability into the skin [29, 33].

To overcome these shortcomings, in this study, HA was selected as a basis material to produce MNs. HA is a water-soluble polymer of disaccharides, naturally found in many tissues of the body, such as skin, cartilage and the vitreous humor. In 2003, the FDA approved HA injections for filling soft tissue defects. Until now, HA was used as a common ingredient in cosmetics to minimize the appearance of facial lines and wrinkles, with effects typically lasting for different times according to the molecular weight of the injected HA. Moreover,

HA has also been added to moisturizers, makeup and soap. It has a high potential to provide desired drug release by using the HAs with different molecular weight. Its high biocompatibility and other physical and chemical properties make it a suitable candidate for the fabrication of microneedles without any heating step. Moreover, the absence of organic solvents and elevated temperatures are notable advantages for preserving peptide and biomolecule stability. Furthermore, the mold-based fabrication process is relatively in expensive and suitable for mass production,in contrast to other published methods that require more complex multistep fabrication schemes.

Based on these findings, HA-fabricated MNs was prepared in this study. In Chapter 1, the piercing and dissolution properties of the MNs in the skin were examined. The disruption and the recovery of skin after their application were further assessed to confirm the safety of these arrays. Moreover, FD4 as a model drug with relatively high molecular weight was loaded in HA-fabricated MNs. It was used to compare the transdermal delivery of FD4 using MNs with a solution formulation *in vitro*. It is generally known that the *in vivo* experimental conditions including pharmacodynamic effects, metabolic activity and blood supply differ from the *in vitro* conditions. Further studies with the MNs containing therapeutic drugs for diabetes were conducted to confirm the potential use in clinical application in Chapter 2.

Insulin medication is currently effective in the treatment of Type I diabetes. Due to the poor absorption or enzymatic degradation of insulin in the gastrointestinal tract and liver, the subcutaneous route has been so far the preferred method of insulin administration. However, this route is associated with poor patient compliance due to the pain caused by injection and risk of inflammation and infection. Consequently, minimally invasive and comfortable routes, including pulmonary, nasal, buccal, and transdermal routes, have been investigated as alternative delivery routes of insulin [34-39]. However, the absorption of insulin from these routes into the systemic circulation is still poor compared to the subcutaneous injection route, and a more effective method of administration is warranted for the delivery of insulin, as well

as other peptide and protein drugs, into the systemic circulation. Therefore, insulin-loaded MNs was prepared with insulin loaded in whole needles in this study. The characteristics of hygroscopy, stability and *in vitro* release were assessed, and the transdermal delivery of insulin was compared with subcutaneous injection route in diabetic rats *in vivo*.

Exendin-4 is the first glucagon-like peptide-1 (GLP-1) receptor agonist to be approved for therapeutic use in humans. This peptide has 39 amino acids originally isolated from the saliva of the gila monster. It shares approximately 53 % sequence homology with the mammalian gut hormone, GLP-1 [40].Due to changes in amino acid sequence, exendin-4 is resistant to degradation against the enzyme dipeptidyl peptidase-4 (DPP-4)[41-43], and has a longer half-life than native GLP-1. As a GLP-1 receptor agonist, exendin-4 shows numerous anti-diabetic actions, including glucose-dependent simulation of insulin secretion [44, 45], suppression of glucagon secretion [45, 46], reduction of gastric mobility and food intake [45-47] and improvement in pancreatic endocrine function [45, 46].Twice-daily subcutaneous injection has been associated with improvements in glycemic control in type 2 diabetic subjects that are inadequately treated with existing antidiabetic agents [48, 49]. However, its therapeutic utility is limited because of the frequent injections required and the associated inconvenience to patients. In addition, drug loading in whole MNs is difficult to accurately control the drug dose delivered to skin because only part of the needle could be inserted into skin due to skin deformation during insertion in many previous studies [50-52]. To address these issues, exendin-4 tip loaded MNs were prepared and exendin-4 was only localized in the needle tips, which can be delivered into skin within short application time despite skin deformation. This allows drug delivery to be controlled and minimizes drug loss. Moreover, drugs with higher concentration MNs can be more quickly delivered to the skin, when compared with drug-loaded whole MNs. Therefore, exendin-4 tip loaded MNs were characterized, and their acute efficacy was compared with subcutaneous injections by intraperitoneal glucose tolerance tests (IPGTTs) in type 2 diabetic GK/Slc rats *in vivo*.

CHAPTER 1 Characteristics of novel microneedle arrays fabricated from hyaluronic acid

Since skin is elastic and deforms during insertion, microneedles with specific physical and geometrical properties are necessary to puncture the skin without breaking. Verbaan et al. reported that unlike 550, 700 and 900 μm microneedles, short (i.e. 300μm) microneedles did not puncture the dermal skin successfully due to the deformation of skin [52]. Thus, to deliver drug deeply into dermis, the HA MNs were designed to have the length of 800 μm which is reasonably long enough to overcome the bulk elastic tissue compression of the skin. Moreover, microneedles with sharp tips might reduce the force needed to puncture the skin, but increased sharpness usually reduces mechanical strength. Previous studies have shown that the strength of microneedles was reduced with an increase in needle length and a decrease in base diameter [32]. To improve mechanical strength, the geometry of tapered-cone shaped microneedles with a base diameter of 160 μm and a tip diameter of 40 μm was designed to expect sufficient mechanical strength for insertion. Additionally, the pitch between needles was chosen to be 600 μm in order to prevent neighboring needles from hindering each other during insertion. One problem in the MN application is that the insertion depth and the insertion ratio of the HA MNs may vary due to the application force and the skin property of different subjects. For reproducible insertion in skin, HA MNs were applied into the skin by an applicator which can apply MNs into the membrane or skin with a definite force (15 N/cm^2).With this applicator, the energy applied on MNs is well controlled, and the force is enough for the consistent insertion of MNs into the skin.

In this study, the penetration capacity of the HA MNs with the design mentioned above was tested in the histological analysis. Moreover, the skin disruption caused by MNs was determined with TEWL and TER measurements. The recovery of insertion site and the skin primary irritation were assessed to confirm the safety of these arrays. Furthermore, FD4 as a

model drug with relatively high molecular weight was loaded in HA-fabricated MNs. It was used to further investigate the enhancement effect on transdermal delivery of FD4 *in vitro*.

1.1. Materials

HA was kindly provided by Shiseido Co., Ltd. (Tokyo, Japan).FD4 was purchased from Sigma-Aldrich Chemical Co. (St. Louis, MO, USA).Tissue-TeK® O.C.T. Compound was purchased from Sakura Finetek Japan Co., Ltd. (Tokyo, Japan). All other chemicals and reagents were of analytical reagent grade.

Male Wistar rats, weighing 220–270g, were purchased from Shimizu Laboratory Supplies Co., Ltd. (Tokyo, Japan). All experiments were performed in accordance with the guidelines of the Animal Ethics Committee at Kyoto Pharmaceutical University.

1.2. Fabrication of hyaluronic acidmicroneedle arrays

1.2.1 Methods

The MNs without any drug material (placebo), and containing blue dye or FD4, were fabricated by micromoulding technologies with HA as a base material. The fabrication process of MNs can be considered as transcription from the micromould with needle-shape in place. In detail, 15 % HA solution was obtained by mixing well with distilled water. Blue dye or FD4 solution was added to the 15 % HA solution and mixed well to prepare HA solution containing blue dye or FD4. 0.1 ml of the resulting HA solution containing blue dye or FD4 was placed on a 2 cm×2 cm micromould at room temperature. After 2 h drying in desiccator, a 2 cm×2 cm PET adhesive tape was attached on the base plate for reinforcing, then 0.1 ml of 20 % HA solution was placed on the PET. After drying completely, a sheet of MNs containing blue dye or FD4 was obtained by peeling the mold off. MNs containing blue dye or FD4 in circular area with a diameter of 10 mm were obtained by cutting the sheet with a punch.

Using this fabrication process, the resulting base plate below PET connected with needles

was considered to consist of HA and blue dye or FD4 with same concentration as that in needles. In the case of MNs containing 5 % (w/v) FD4, the total amount of FD4 is 250 µg, including 50 µg in needles and 200 µg in base plate.

1.2.2. Results and Discussion

Fig.1 A and B show the overall and magnified view of the MNs fabricated from HA by a video microscope. They were designed to have 190 microneedles in a circular array with a diameter of 10 mm. Needles were tapered cone-shaped and of uniform dimension. Each needle was approximately 800 µmin height, and had a diameter of 160 µm at the base and 40 µm at the tip. The rows of needles for the MNs were spaced at a distance of 600 µm.

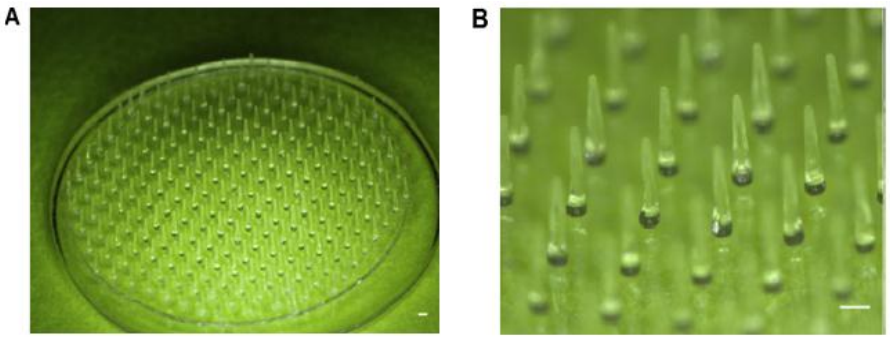

(European Journal of Pharmaceutics and Biopharmaceutics, Fig.1)

Fig.1. (A) MNs observed by a video microscope and (B) image of a portion of the microneedles with a length of 800 µm, a diameter of 160 µm at the base and 40 µm at the tip. Bars = 200 µm.

1.3. Penetration capacity of hyaluronic acidmicroneedle arrays

1.3.1. Methods

MNs were used for insertion into human cadaver skin and left in place for 5 min. Upon removal of the MNs, the skin sample was subsequently embedded in OCT compound. The

samples were then frozen in dry ice and acetone (−78 °C) and sectioned into 10-µm-thick slices using a cryomicrotome (Histostat Cryostat Microtome, Buffalo, NY, USA). The skin sections were stained with H&E and examined using a bright-field microscope (BZ-8000, Keyence, Osaka, Japan) to observe the pathway created by the microneedle.

1.3.2. Results and Discussion

To confirm the puncturing property of MNs, the cross-section of skin was observed after MNs insertion.Fig.2A shows the histological cross-section of untreated skin after H&E staining, which assists with visualization of skin architecture. The outermost layer of skin is the stratum corneum and the underlying thin layer is the epidermis, which is seen atop a thick layer of dermis. As shown in Fig.2A, a drug permeation pathway is non-existent before the application of the MNs. Fig.2 B shows the cross-section of the skin after the application of the MNs. After being inserted into the dermis, they created drug permeation pathways that had a similar shape to the inserted MNs. Moreover, as shown in Fig.2C, the MNs insert into skin with a distance similar to the pitch of microneedles, indicating that the MNs were uniformly inserted. The incision created by MNs is found to be approximately 130 µm, and the depth of the incision is at least about 300 µm. The effective penetration is found to be shorter than the total length of the microneedles, which has also been mentioned in previous papers [50, 51]. However, the incision dimensions above may be underestimated because the skin is elastic and may retract during preparation of skin sections after microneedle removal.

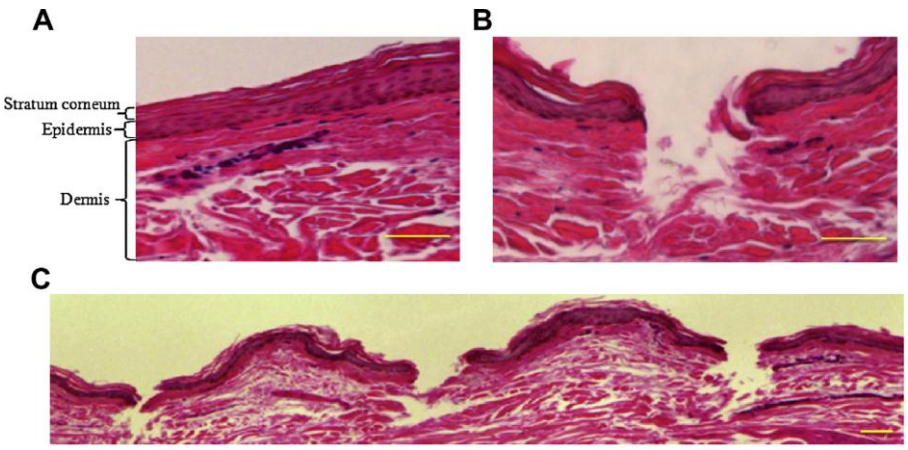

(European Journal of Pharmaceutics and Biopharmaceutics, Fig.2)

Fig.2. (A) Untreated skin section after H&E staining. (B) and (C) Microneedle-treated skin section after H&E staining. Bars = 100 μm

1.4. Visualization of micropores created by insertion of microneedle arrays

1.4.1. Methods

MNs containing blue dye were applied to the rat skin and left in place for 1 h *in vivo*. After removal, pictures of the treated skin site were taken using a digital camera to confirm the uniformity of the insertion.

1.4.2. Results and Discussion

To confirm the uniform insertion of MNs, the surface of the test site after insertion was observed. Fig.3A shows the surface of rat skin after insertion of the MNs containing blue dye. Fig. 3B indicates the microscope images of MNs containing blue dyes after 1 h application in rat skin. Needles were completely dissolved within 1 h, and the application site was stained by blue dye released from microneedles. Moreover, the blue dots corresponded to the application sites of the MNs. No breakage or residue of needles was observed on the skin surface. These findings indicated that the blue dye loaded HA MNs have sufficient mechanical strength for insertion and uniformly created pathways that the drug was

successfully delivered into the skin.

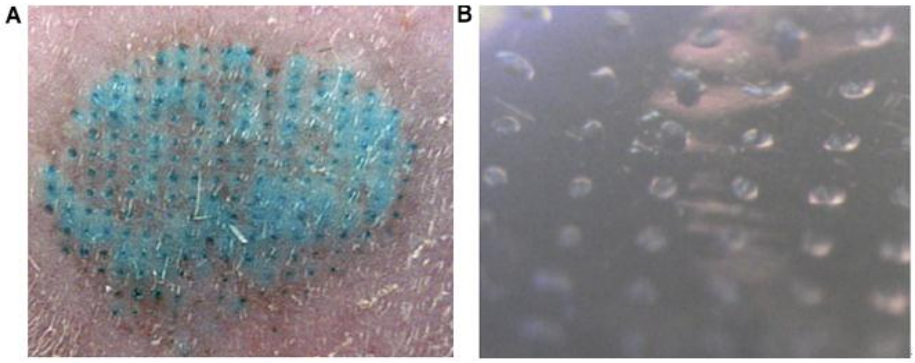

(European Journal of Pharmaceutics and Biopharmaceutics, Fig.3)

Fig.3. (A) Photograph of rat skin after insertion of MNs containingblue dye and (B)microscope image of MNs containing blue dye after1 h application in rat skin.

1.5. Diffusion of FD4 in human skin with microneedle arrays containing FD4

1.5.1. Methods

The diffusion of FD4 from the MNs in human cadaver skin was observed in order to assess the microneedle-media transdermal drug delivery. MNs containing 5 % FD4 were inserted into human cadaver skin for 1 h. After removal, the skin sections were obtained by the same process mentioned above in 1.2.2 and examined by an all-in-one fluorescence microscope (BZ-8000, Keyence, Osaka, Japan).

1.5.2. Results and Discussion

Figs. 4A and B show cross-sections of human skin untreatedand treated with MNs containing 5 % FD4. Collectively, these observations suggested that themicroneedles successfully delivered FD4 into the skin and that the deposition of FD4 was localized to the resulting microchannels. Moreover, most fluorescence was observed to be along the shaft of the insertion path. The nearer to the incision, the higher intensity was observed. These

findings indicate that, along with the dissolution of the needles, FD4 was released from the soluble MNs and delivered to the skin by diffusion.

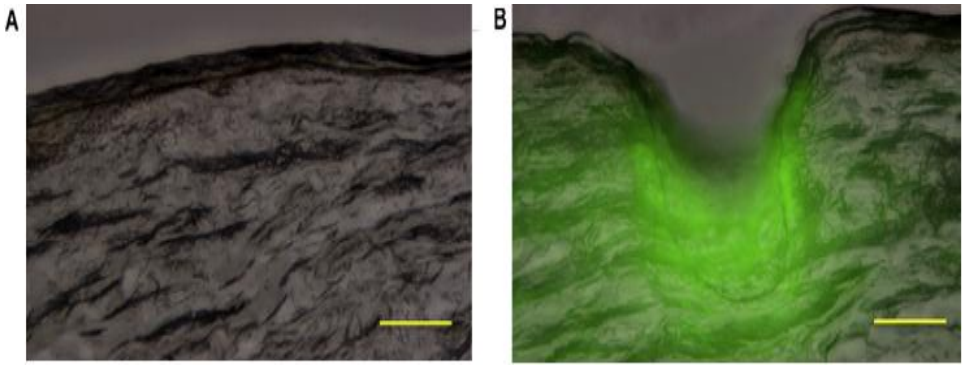

(European Journal of Pharmaceutics and Biopharmaceutics, Fig.2)

Fig.4. (A) Fluorescence microscopy image of untreated skin section. (B) Fluorescence microscope image of skin section after application of 5 % (w/v) FD4-loaded MNs for 1 h. Bars = 100 μm

1.6. Dissolution of microneedle arrays in rat skin

1.6.1. Methods

Rats were anesthetized and abdominal skin was shaved prior to the initiation of the experiment. HA MNs were then applied onto abdominal skin and fixed with a gum tape. At indicated time intervals, HA MNs were removed from the skin sites and visualized with light microscopy.

1.6.2. Results and Discussion

Fig. 5 demonstrates the bright micrographs of MNs before and after their application onto rat skin *in vivo* at 5 min, 30 min, 1 h, 2 h and 7 h. MNs appeared to successfully pierce through rat skin without any bending or cracking and started to dissolve at 5 min. It is also evident from Fig. 5 that approximately 3/4 of the total length was dissolved at 30 min, all of

the needles were completely dissolved within 1 h and the base plate started to be dissolved after the application at 2 h. Moreover, continuous dissolution of the base plate was seen after application at 7 h. Therefore, the novel HA MNs appear to have self-dissolving properties and are easily dissolved upon application to skin.

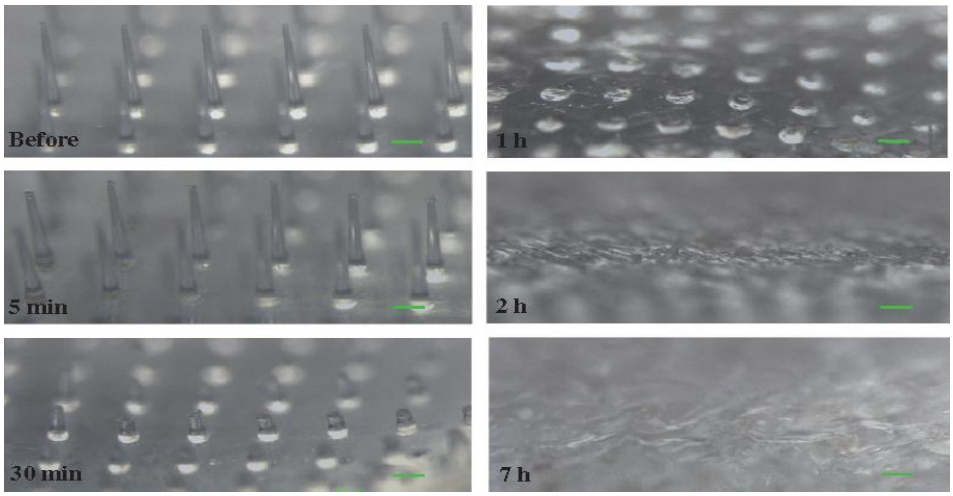

(European Journal of Pharmaceutics and Biopharmaceutics, Fig.4)

Fig.5. Dissolution of MNs after their application onto rat skin *in vivo* at the indicated time points. Bars = 200 μm

1.7.Determination of transepidermis water loss

1.7.1. Methods

Since shaving the skin may possibly compromise the stratum corneum, the back skin of rats was shaved 24 h prior to the experiment. Just before the application, healthy rats without signs of illness were chosen and their skin without scratch or wound was confirmed to be normal. After confirmation of skin site, rats were anesthetized with an intraperitoneal injection of 45 mg/kg pentobarbital sodium and acclimated in ambient conditions for 1 h (room temperature of 25 °C and a relative humidity of 50 %). TEWL was measured with a Tewameter (TM 300, Courage and Khazaka Electronic GmbH, Cologne, Germany) at skin

sites without any treatment (control group), skin sites applied with HA MNs (MN group) and skin sites treated with sequential tape-stripping 15 times using adhesive cellophane tape (TS group). The MNs with approximately 190 needles in the circular area with a diameter of 10 mm were used in the MN group. The treated area of TS group was the same as the treated area of MN group (a circular area with a diameter of 10 mm). TEWL was measured before treatments and at 0, 15, 30, 60 and 90 min after treatments in all groups.

1.7.2. Results and Discussion

The measurement of TEWL is a standard method of determining changes in skin barrier properties, and is frequently used in dermatological and cosmetological fields [53, 54]. This method allows researchers to uncover disruptions in the skin barrier during early stages of development, even before they are noticeable. Recently, the TEWL has been used to evaluate the integrity of skin after the application of MNs [52, 55, 56].Therefore, to assess the puncturing properties, TEWL of the injection sites was measured in the study. Before treatment, TEWL of intact skin was approximately 15.8 ±1.1 g h^{-1} m^{-2}. As shown in Fig.6, immediately after treatment, a significant increase in TEWL was observed in both the MNs ($P<0.01$) and tape stripping ($P<0.001$) groups, compared with the control group. The maximum percent change in TEWL was observed in the tape stripping group with a value of 492.0 ± 62.3 %. However, TEWL did not decrease after the tape stripping treatment over the course of the experimental period, suggesting that the effects of tape stripping might be irreversible. On the other hand, after insertion of the MNs into the skin, TEWL also increased to 293.8 ± 35.9% of the baseline value. However, the percent increase in TEWL was much lower than that observed in the tape stripping group. These findings demonstrated that the MNs successfully punctured the skin and that the extent of disruption caused by MNs was relatively small, as compared to tape stripping. This finding is well correlated with the results of previous reports [52, 57]. Although the TEWL did not completely recover to the baseline

values within 90 min in the MN group, a decreasing tendency for TEWL was found during the experimental period. It may be that the pore size created by MNs is reduced gradually after the removal of MNs. This notion was, in fact, previously confirmed by light and scanning electron microscopy [58]. Furthermore, according to a report by Wang et al. [17], the reduction in pore size may be faster in the *in vivo* condition due to the physiological response of skin. These findings indicate that the novel MNs did not seriously damage the skin and were quite safe compared with tape stripping.

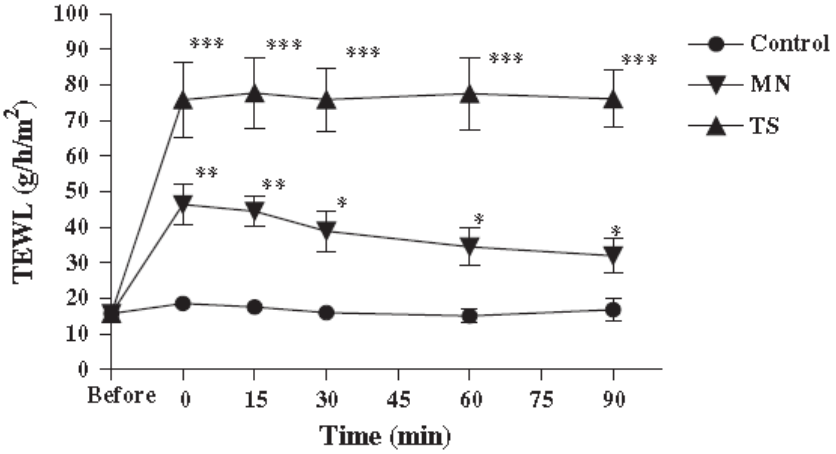

(European Journal of Pharmaceutics and Biopharmaceutics, Fig.5)

Fig.6. Effects of the MNs and tape stripping treatment on TEWL of rat skin *in vivo* at the indicated time point compared to intact skin (control). Results are expressed as mean ± SE of 9 experiments. (***) $P < 0.001$, (**) $P < 0.01$, (*) $P < 0.05$, compared with the control.

1.8.Determination of transcutaneous electrical resistance

1.8.1. Methods

Rats were anesthetized with an intraperitoneal injection of 45mg/kg pentobarbital sodium and their back hair was shaved 24 h before the test. Since shaving the skin may possibly compromise the stratum corneum, healthy rats without signs of illness were chosen and their skin without scratch or wound was confirmed to be normal. After checking skin site, the skin

electrical resistance values were measured with a Pocket Tester (CDM-03D, Custom, Tokyo,Japan) at skin sites without any treatment (controlgroup), skin sites applied with MNs (MN group) and skin sites treated with tape stripping (TS group).The treatments with MNs andtape stripping were the same as those for the TEWL test. TER was determined before and directly after removing MNs and repeated at the indicated times by placing the electrodes onto the skin until a stable reading was obtained.

1.8.2. Results and Discussion

TER is another method to evaluate skin integrity and is determined by measuring the passage of an electrical current across the skin [59-61]. The stratum corneum is known to be a poorly conductive dielectric medium and resistant to ion flow. Ions move easily across damaged skin due to low barrier function, resulting in a decrease in TER. Prior to the treatment, TER of intact skin was approximately 41.8 ± 0.4 $M\Omega \bullet cm^2$. Fig.7 shows that TER was significantly reduced after treatment in both the MN ($P < 0.01$) and tape stripping ($P < 0.001$) groups, compared with the control group. The approximate 40 % decrease in TER from the initial value was observed after the tape stripping treatment, and TER reached a plateau and did not recover to baseline values during the experimental period. On the other hand, the MNs caused an approximate 15 % decrease in TER. Moreover, TER increased after removal of the MNs and recovered to the baseline value at 30 min. Therefore, decreased TER after application of MNs appeared reversible. Different recovery time between TER and TEWL measurement may be due to the difference in their principles of measurements. Unlike TEWL, the change in TER is more correlated with the extent of disruption on stratum corneum which forms a high-electric resistance layer, and the resistance of this layer was found to become low toward the inner part [62].

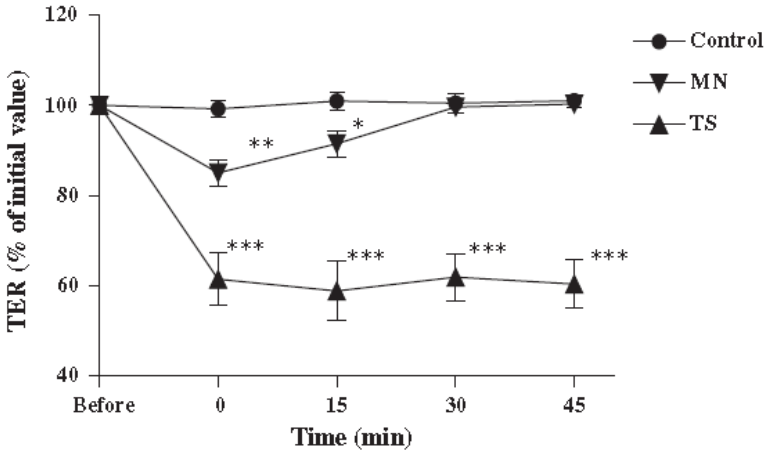

(European Journal of Pharmaceutics and Biopharmaceutics, Fig.6)

Fig.7. Effects of the MNs and tape stripping treatment on TER of rat skin *in vivo* at the indicated time point compared to intact skin (control). All results are expressed as percent change in TER relative to initial value. Results are expressed as mean ± SE of 6–8 experiments. (***) $P < 0.001$, (**) $P < 0.01$, (*) $P < 0.05$, compared with the control.

1.9. Skin primary irritation test

1.9.1. Methods

A Draize test [63] was selected to observe the presence of erythema and edema on the skin sites applied with MNs. The back skin of rats was shaved 24 h prior to the experiment. Just before the application, healthy rats without signs of illness were chosen and their skin without scratch or wound was confirmed to be normal. The MNs and base plates without arrays were then applied to the skin for 2 h. Upon removal, scoring of the erythema and edema was performed at 1 h, 24 h and 72h with the Draize dermal scoring criteria. The Primary Irritation Index (P.I.I.) was calculated according to the following equation.

$$P.I.I. = \frac{\sum \text{Erythema grade at 1 h, 24 h and 72 h} + \sum \text{Edema grade at 1 h, 24 h and 72 h}}{\text{number of rats} \times \text{number of application skin sites} \times \text{time of reading}}$$

The irritancy potential of the MNs was evaluated according to the Draize dermal scoring criteria, as described below.

The Draize dermal scoring criteria

P.I.I.	Classification
0.0–0.4	No irritation
0.5–1.9	Slight irritation
2.0–4.9	Moderate irritation
5.0–8.0	Severe irritation

1.9.2. Results and Discussion

Draize test is commonly used to evaluate cosmeceutical, pharmaceutical and environmental chemical substances. Due to the fact that the MNs were completely dissolved in rat skin within 1 h *in vivo*, the application time of the MNs was extended to 2 h, which is long enough to dissolve the MNs thoroughly in the skin and thus evaluate the degree of primary irritation. In the skin irritation test, the scores for erythema and edema from the skin sites treated with MNs were evaluated for all rats at 1 h, 24 h and 72 h. As shown in Fig.8A, slight erythema but no edema was evident at the injection sites at 1 h and disappeared within 24 h. The P.I.I. of the MNs was calculated to be 1.7, confirming a low degree of skin irritation. Fig.8B shows photograph of the site of skin at 1 h, 24 h and 72 h after removal of base plate without microneedles. As shown in Fig.8B, slight redness was also seen on the skin site at 1 h and disappeared at 24 h and 72 h after removal of the base plate. It indicates that the erythema was most likely induced by a vasodilatation response to the physical compression of the dermis during application of the MNs rather than by the irritation caused by the HA material or the MNs themselves. In addition, it is known that rat skin is thinner than human skin, so that the erythema induced by physical compression of the dermis by MNs in the case of human skin is reasonably much slighter than that induced in rat skin *in vivo*. Therefore, these findings indicated that irritation and skin damage caused by HA MNs were slight and transient, which is consistent with TEWL and TER results.

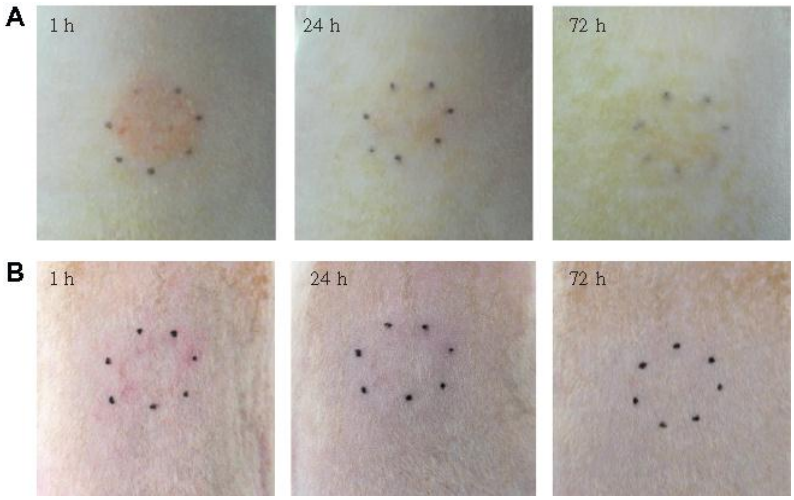

(European Journal of Pharmaceutics and Biopharmaceutics, Fig.7)

Fig. 8.(A) Photograph of the sites of rat skin at 1 h, 24 h and 72 h after the removal of MNs and (B) photograph of the sites of rat skin at 1 h, 24 h and 72 h after the removal of base plate without arrays.

1.10. *In vivo* dermatoscope observation

1.10.1. Methods

Back skin of Wistar rats was shaved 24 h prior to the experiment. Just before application, healthy rats were selected and skins in normal sections were used for subsequent studies. MNs were inserted into skin and left in place for 5 min. For comparison, subcutaneous injection using a 26 G needle was manually conducted in the skin. After removal of the MNs and subcutaneous injection with a 26 G needle, test sites were observed at 0 h, 24 h and 72 h with a Dermatoscope (DermaShot-Scope; Fineopto, Kyoto, Japan).

1.10.2. Results and Discussion

In order to estimate the disruption and recovery of skin by the MNs, skin injury and damage after the application of MNs were compared with that after subcutaneous injection with a 26 G needle using a dermatoscope. Fig.9 shows the surface images of rat skin after

insertion of MNs and subcutaneous injection with a 26 G needle. The number of the pores created by MNs was much greater than the one pore created by subcutaneous injection, but the pore size was much smaller. In the microneedle-treated group, pores corresponding to MNs were observed on test skin sites after removal of MNs. These pores gradually reduced with time and had almost disappeared at 24 h after application. In contrast, pores created by subcutaneous injection with a 26 G needle were clearly observed, even at 72 h after application, although they were smaller when compared to 24 h after application. Based on these findings, the MNs were confirmed not to cause serious skin damage or irritation, and that they were safe after application. Moreover, even though MNs were degraded in the skin, they were very safe, as they were composed of hyaluronic acid, an endogeneous biodegradable substance.

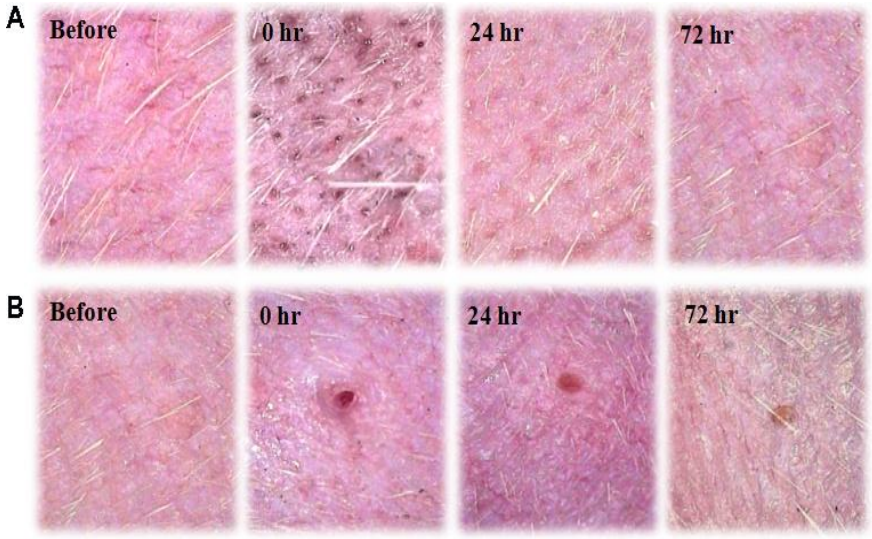

Fig.9 Dermatoscopy of rat skin before and at 0 h, 24 h and 72 h after treatment with MNs (A) and subcutaneous injection with a 26 G needle (B).

1.11. *In vitro* transdermal delivery of FD4 by hyaluronic acid microneedle arrays

1.11.1. Methods

In vitro permeation studies were carried out with Franz diffusion cells with an effective

diffusion area of 3.14 cm^2. Human cadaver skin with thickness of about 1mm was cut into 30-mm-diamter circles and placed (stratum corneum uppermost) onto an identically sized circular piece of filter paper. In the MNs group, MNs containing 5 % (w/v) FD4 were applied to the human cadaver skin. These skin membranes with the MNs in place were subsequently clamped between the receptor and donor compartments of cells with the stratum corneum facing the donor compartments. In the solution group, 5 % (w/v) FD4 solution was applied to the intact skin mounted between the receptor and donor compartments without any microneedle treatment. After application of the samples, the receptor compartments were slightly tilted and filled with 2.4 ml of phosphate buffer (pH 7.4, PBS) and stirred with magnetic bars. During the transdermal delivery studies, air bubbles beneath the skin samples were confirmed not to exist in each cell. The temperature was maintained at 32 °C. The receptor solution (500 μl) was withdrawn at the indicated time and replaced with an equal volume of a fresh receptor solution. Samples were stored in a refrigerator at 4 °C until analysis was performed.

The amount of FD4 permeated in the stratum corneum was then determined. Adhesive cellophane tape stripping was performed on the stratum corneum 15 times after removal of the test materials. The first strip of peeled tape was discarded because of the residual material left on the surface of the stratum corneum. The second through the fourteenth tape strips were collected and put into a 50 ml centrifuge tube. FD4 was extracted from these tape strips with 15 ml of PBS and1 h of sonication. The extraction solution was transferred to a 100 ml beaker and the solvent was evaporated completely in a 70 °C water bath. PBS (1 ml) was used to re-dissolve the extracted FD4. After the samples were centrifuged at 10,000 rpm (7,710×g) for 5 min, the supernatant was stored in a refrigerator at 4 °C until analysis was performed.

FD4 permeated in the epidermis and dermis was also determined. After tape stripping, skin pieces were cut into smaller pieces and homogenized in 5 ml of distilled water. Ethanol (15 ml) was added to the skin homogenate to extract FD4. After the samples were centrifuged at

5,000 rpm (4,000×g) for 5 min, the extraction solution was collected and transferred to a 100 ml beaker. The solvent was evaporated completely in a 70 °C water bath, and 1 ml of PBS was used to re-dissolve the extracted FD4. After the samples were centrifuged at 10,000 rpm (7,710 ×g) for 5 min, the supernatant was stored in a refrigerator at 4 °C until analysis was performed.

FD4 was analyzed on a fluorescence HPLC system (Hitachi, Tokyo, Japan). Samples were eluted on a C18 column (5C18-AR-Ⅱ, 4.6×150 mm, Nacalai Tesque, Kyoto, Japan) using a mobile phase consisting of 0.1 % phosphoric acid and acetonitrile (80:20). A flow rate of 1 ml/min was maintained. The excitation wavelength was 485 nm and the emission wavelength was 585 nm. All statistical analyses were performed using GraphPad Prism software (GraphPad Software Inc., San Diego, CA, USA). Descriptive statistics are presented as mean values ± SE. Unpaired or paired Student's *t*-tests were applied for comparisons between or within the same group, respectively. For all comparisons, $P<0.05$ was considered to be statistically significant.

1.11.2. Results and Discussion

To evaluate the transdermal delivery of drugs with relatively high molecular weight by MNs, HA MNs containing FD4 were prepared and compared the permeation of FD4 across human cadaver skin with that in FD4 solution. Fig.10 shows the *in vitro* cumulative permeated amount of FD4 after application of MNs containing FD4 or FD4 solution. As indicated in Fig.10, the cumulative permeated amount of FD4 significantly increased across the skin after the application of MNs compared to the solution over a period of 7 h. The cumulative permeated amount of FD4 in solution was low, with a value of 0.38 ± 0.20 μg/cm^2. In contrast, the cumulative permeated amount of FD4 increased significantly after application of MNs with a value of 231.80 ± 28.76 μg/cm^2 over the same period. It indicates that the novel MNs were effective in improving the transdermal permeability of FD4 as a model drug

with relatively high molecular weight. In addition, almost no lag time was observed in drug permeation of the MN group. It correlated well with the results from previous studies [6, 25]. This interpretation was confirmed by histological sections in our study as mentioned above, which showed that the MNs inserted into the dermis directly delivered FD4 into the skin.

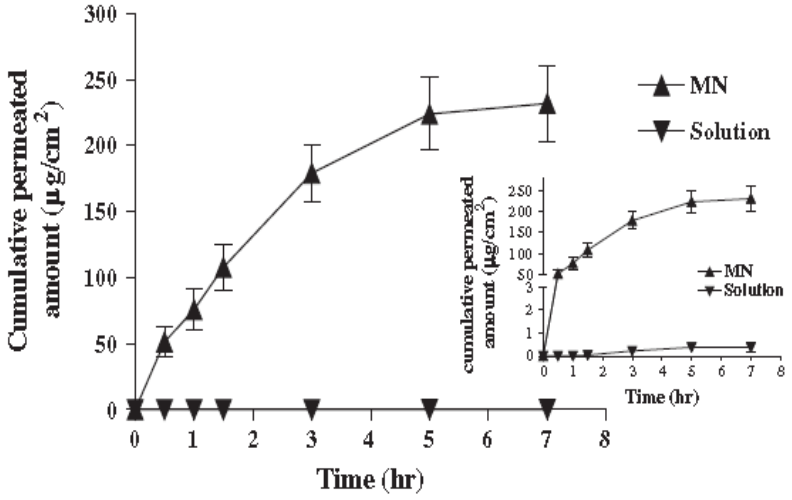

(European Journal of Pharmaceutics and Biopharmaceutics, Fig.8)

Fig.10. *In vitro* cumulative permeated amount of FD4 after application of MNs containing FD4 or application of FD4 solution over a period of 7 h. Results are expressed as mean ± SE of 3–4 experiments.

Fig.11 shows the amount of FD4 that permeated into the stratum corneum, epidermis and dermis and receptor compartment after the application of MNs containing FD4 or FD4 solution, over the transdermal delivery period of 7 h. With the MNs, the total amount of permeated FD4 was 278.74 ± 36.15 μg/cm^2, approximately 87.5 % of the total amount of FD4 (250 μg in the microneedle arrays with the diameter of 10 mm, including 50 μg in needles and 200 μg in base plate). It increased in the following order: stratum corneum<epidermis and dermis <receptor compartment. In contrast, a marginal amount of FD4 permeation was observed after application of the FD4 solution with a value of 2.53 ± 0.81 μg/cm^2,

approximately 3 % of the total amount of FD4. In this case, FD4 only permeated across the stratum corneum and localized in the outer layer of the skin. Almost no transport of FD4 was found in the epidermis and dermis and receptor compartment after the application to the skin. Therefore, MNs were much more effective for increasing the accumulation of drug with relatively high molecular weight in the skin.

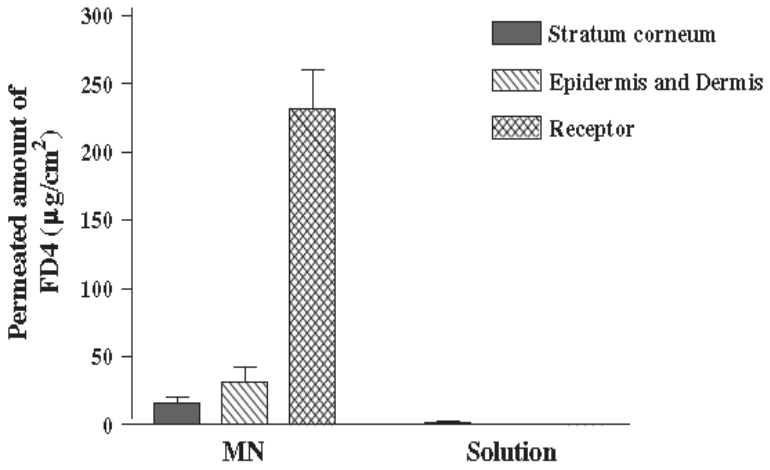

(European Journal of Pharmaceutics and Biopharmaceutics, Fig.9)

Fig.11. Permeated amount of FD4 into the stratum corneum, epidermis and dermis and receptor compartment for 7 h after application of the MNs containing FD4 or application of FD4 solution. Results are expressed as mean ± SE of 3–4 experiments.

CHAPTER 2 Application in the transdermal delivery of diabetes drugs

The capacity limitation of HA MNs depends on physiccochemical properties of the compound contained when mixed with HA. Based on our experience on the production of the HA MNs containing alendronate, FD4 and insulin, the capacity limitation was at least 10 %, which was equal to about 5 mg/cm^2 when the drug is loaded in whole MNs. This amount is sufficient to deliver most drugs including the insulin and the exendin-4 for the treatment of diabetes at therapeutic dose. Moreover, the delivery capacity of the MNs could be further adjusted by increasing the application area and dosing frequency due to the low damage to skin. As mentioned earlier, one problem of HA MNs application is that the insertion depth and the insertion ratio of the HA may vary due to application force and skin property of different subjects. However, as mentioned on page 10, using the applicator to well control the energy applied on microneedles can overcome the problem and provide consistent insertion in skin.

The studies in Chapter 1 focus on safety and enhancing transdermal permeation of drugs via MNs without evaluating the characteristics of MNs, which is of particular importance in clinical applicability. In the present study, the characteristics of MNs, including drug contents, hygroscopy, drug stability at various storage conditions and drug releasing profiles from a clinical application point-of-view. As *in vivo* experimental conditions including pharmacodynamic effects and metabolic activity differ from the *in vitro* conditions, insulin loaded MNs and exendin-4 tip-loaded MNs were further compared with subcutaneous injections in transdermal delivery of insulin and exendin-4 to diabetic rats *in vivo* in this study.

2.1. Materials

HA was kindly provided by Shiseido Co., Ltd (Tokyo, Japan). FD4 and streptozotocin was purchased from Sigma-Aldrich Chemical Co. (St. Louis, MO, USA). Pentobarbital sodium,

citric acid buffer solution, and bovine insulin (28 IU/mg)were purchased from Nacalai Tesque Inc. (Kyoto, Japan). Exendin-4, Glucose CII test kits and insulin-EIA test kits were purchased from Wako Pure Chemical Industries, Ltd. (Osaka, Japan). Rat Insulin ELISA kits were purchased from Shibayagi Co., Ltd. (Gunma, Japan).Exendin-4 EIA kits were purchased from Phoenix Pharmaceuticals, Inc. (Belmont, CA). All other chemicals and reagents were of analytical reagent grade.

Male Wistar rats (weighing 220-270 g) and male GK/Slc rats (aged 7~8 weeks and weighing 190-200 g) were purchased from Shimizu Laboratory Supplies Co., Ltd. (Kyoto, Japan). All experiments were performed in accordance with the guidelines of the Animal Ethic Committee at Kyoto Pharmaceutical University.

2.2 Application in the transdermal delivery of insulin with insulin-loaded microneedle arrays

2.2.1. Fabrication of insulin-loaded microneedle arrays

2.2.1.1 Methods

0.13, 0.25, and 0.44 IU of bovine insulin loaded MNs were fabricated via micromolding technologies with HA as the base material. The fabrication process of MNs can be considered as transcription from the micromould with needle-shape in place. In detail, 15 % HA solution was obtained by mixing well with distilled water. Insulin solution dissolved in 0.1 M HCl solution was added to the 15%HA solution and mixed well to prepare HA solution containing insulin. 0.3 ml of the resulting HA solution containing insulin was placed on a 2 cm x 2 cm micromould at room temperature. After 2 h drying in desiccator, the remaining solution was removed on the surface of mould with cotton, then 0.1 ml of 20 % HA solution was placed on the same place of micromould. After drying the micromould completely, a 2 cm x 2cm PET adhesive tape was attached on the baseplate for reinforcing. A sheet of insulin-loaded MNs

was obtained by peeling the mold off. Insulin-loaded MNs in circular area with a diameter of 10 mm were obtained by cutting the sheet with a punch. Recording to the fabrication process, the baseplate was considered to consist of HA and a small amount of insulin. The amount of insulin in needles and baseplate was determined, and more than 90% of insulin was detected in the needles. Scanning electron microscopy was performed to examine the MNs.

2.2.1.2 Results and Discussion

A scanning electron micrograph of a section of insulin-loaded MNs fabricated from HA is presented in Fig. 12. The resulting tapered-cone insulin-loaded MNs were uniform in size with sharp tips. Each needle was approximately 800 μm in height, with a diameter of 160 μm at the base and 40 μm at the tip, and an interspacing of 600 μm between the rows of needles. There were approximately 190 needles in a circular area with a diameter of 10 mm. It is found that the incorporation of insulin into HA MNs didn't change the dimension of MNs compared with HA MNs. It indicates that HA as the main material has good integration with the drug loaded in MNs.

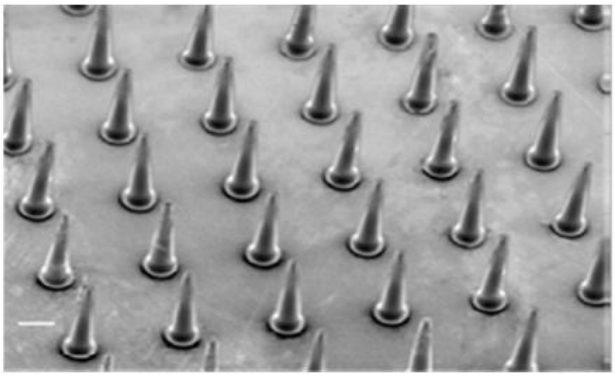

(Journal of Controlled Release, Fig.1)

Fig. 12.Scanning electron micrograph of a section containing insulin-loaded MNs with lengths of 800 μm, and diameters of 160 μm at the base and 40 μm at the tip. Bar=200 μm.

2.2.2. Determination of insulin contents in insulin-loaded microneedle arrays

2.2.2.1. Methods

0.13, 0.25, and 0.44 U of bovine insulin loaded MNs were weighed and dissolved in 10 ml of pH 7.4 PBS followed by 30 min of sonication. Insulin extracted from MNs was analyzed on a gradient HPLC system (HitachiL-7000, Kyoto, Japan) equipped with a UV detector (Hitachi L-7450, Kyoto, Japan)and a reversed phase column (ODS 5 μm, 4.6 mm x 150 mm, Nacalai Tesque Inc., Kyoto, Japan). The following mobile phase systems were used: A) 0.1 % TFA in H_2O, and B) 0.1 % TFA in methanol. A linear gradient elution from 40 % to 80 % with phase B was performed over 20 min. A flow rate of 1ml/min was maintained, the column temperature was 40 ºC, and the detection wavelength was 210 nm.

2.2.2.2. Results and Discussion

The amount of insulin in insulin-loaded MNs is presented in Table 1.Insulin amount is not significantly altered after production. It was precisely loaded in MNs in accordance with each dosage with the standard error below ± 2 % in all groups.

Table 1 The amount of insulin in the insulin-loaded MNs

Insulin dose (IU/MN)	Percentage of amount (%)
0.13	105.53 ± 1.44
0.25	103.44 ± 0.83
0.44	95.93 ± 1.13

Results are expressed as the means ± S.E. of 3 experiments.

2.2.3. Hygroscopy of insulin-loaded microneedle arrays

2.2.3.1. Methods

Insulin-loaded MNs were stored at a high relative humidity of 75%. This condition was obtained by storing the MNs in a desiccator containing a saturated solution of sodium chloride. MNs were removed at pre-determined intervals, and the weight of MNs was measured and the percent change in MNs weight was calculated. No MN was returned into the container after testing.

2.2.3.2. Results and Discussion

Donnelly et al. reported that galactose MNs had an increasing adhesive nature at a relative humidity of 43%, and that no MN remained after 1 h at a relative humidity of 75% [29]. These findings suggest that MNs fabricated from soluble materials, such as galactose, are unstable at ambient relative humidities. Given that moisture had a great effect on the morphology and mechanical strength of soluble MNs, the hygroscopy of insulin-loaded MNs was evaluated at the high relative humidity of 75% over a 24 h period. As shown in Fig. 13, the percent change in the weight of MNs increased rapidly during the first 7 h, and then slowed down from 7 to 24 h. Furthermore, at a relative humidity of 75 %, it appears that the weight of MNs becomes saturated at approximately 15 % above its baseline weight. The increase in MNs weight due to the absorption of moisture from the wet environment resulted in a softening of HA materials, and thereby a decrease in their mechanical strength. It is the other problem in HA MNs application besides the insertion problem mentioned earlier. However, a sealed packaging is able to solve the problem to protect the MNs. Moreover, MNs were considered to have enough mechanical strength to sufficiently pierce through skin when their increase in weight did not exceed 5 % (data were not shown).These findings suggested that MNs could maintain their insertion ability for at least 1 h even at a relative humidity of 75 %, suggesting that they may be useful in the practical application of MNs. Additionally, the structure of MNs did not change over the experimental period at a relative humidity of 75 %.Therefore, normally the HA MNs is requested to be applied on skin within 1 hour after

taking out from the package.

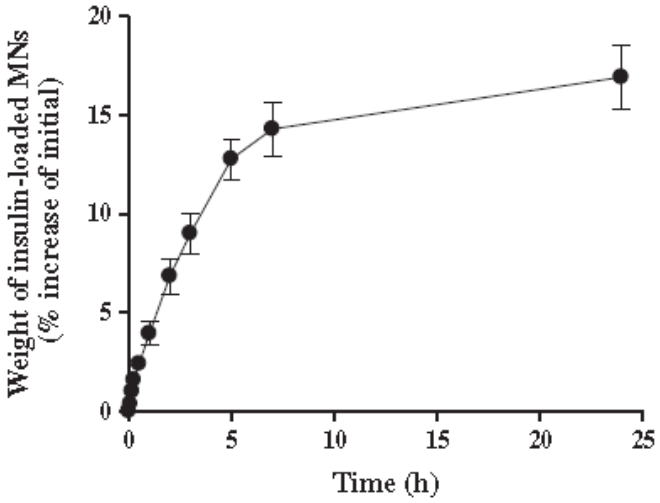

(Journal of Controlled Release, Fig.2)

Fig.13. Hygroscopic profile of insulin-loaded MNs during storage at a relative humidity of 75 %. Results are presented as the mean ± S.E. of 4 experiments.

2.2.4. Stability of insulin-loaded microneedle arrays

2.2.4.1. Methods

Insulin-loaded MNs were stored at -20, 4, 20, and 40ºC for a month. Thereafter, the insulin that remained in the MNs was extracted by the dissolution of the needles in 1 ml of pH 7.4 PBS. Insulin was analyzed with the gradient HPLC assay method as described above.

2.2.4.2. Results and Discussion

The stability of loading insulin into MNs and storing them at −20, 4, 20, and 40 °C is presented in Table 2. It was found that insulin-loaded MNs were not substantially degraded after a month of being stored. More than 90 % of the loaded insulin remained in the MNs after a month of storing them at all four temperatures. There were no statistical differences in the remaining % of insulin loaded in MNs among these different storage conditions, although the stability of insulin at 20 °C was slightly less than that at 40 °C. These findings suggested

that insulin-loaded MNs are stable for at least one month at these storage conditions. Lee et al. previously reported that lysozyme encapsulated in carboxymethylcellulose MNs, which was stable after two months of being kept at room temperature [27]. Consequently, the investigators speculated that the MNs decreased the degradation of lysozyme, and thereby increased its stability [64]. Perhaps for the same reason, the stability of insulin in our study was maintained by the HA MNs at the tested storage conditions. However, future studies that confirm whether the insulin contained within the HA MNs is stable for longer storage periods are warranted.

Table 2 Stability of insulin-loaded MNs after storing for a month at -20, 4, 20, and 40 °C

Temperature (℃)	Insulin remained in MNs (% of initial)
−20	94.82 ± 5.56
4	93.51 ± 5.67
20	90.33 ± 5.54
40	96.19 ± 5.63

Results are presented as the mean ± S.E. of at least 4 experiments. (Journal of Controlled Release, Table 1)

2.2.5. *In vitro* release of insulin from microneedle arrays

2.2.5.1. Methods

The release of insulin from insulin-loaded MNs across Silescol® membranes was investigated by using *in vitro* modified Franz cells. Insulin-loaded MNs were applied onto the centers of the membranes. With the MNs in place, the membranes were mounted onto Franz cells. The cells were positioned upright, and the receptor compartments were filled with 2.4 ml of pH 7.4 PBS and maintained at 32ºC throughout the test period. At pre-determined intervals, 0.5 ml of the supernatant was withdrawn and replaced with an equal volume of

fresh medium. The gradient HPLC assay method was used to detect insulin, as described above.

2.2.5.2. Results and Discussion

The cumulative release of insulin from insulin-loaded MNs was determined via an *in vitro* release study in Fig. 14. At the start of the experiment, MNs were readily dissolved and insulin was rapidly released from the MNs at a relatively constant rate. In the present study, the majority of the insulin was released within 1 h, suggesting that MNs are rapidly and completely dissolved *in vitro*. It is consistent with the *in vivo* dissolution study in Chapter 1, which shows that the novel HA MNs fully dissolved on rat skin within 1 h. These findings indicate that insulin is rapidly released from insulin-loaded MNs fabricated from HA both *in vitro* and *in vivo*.

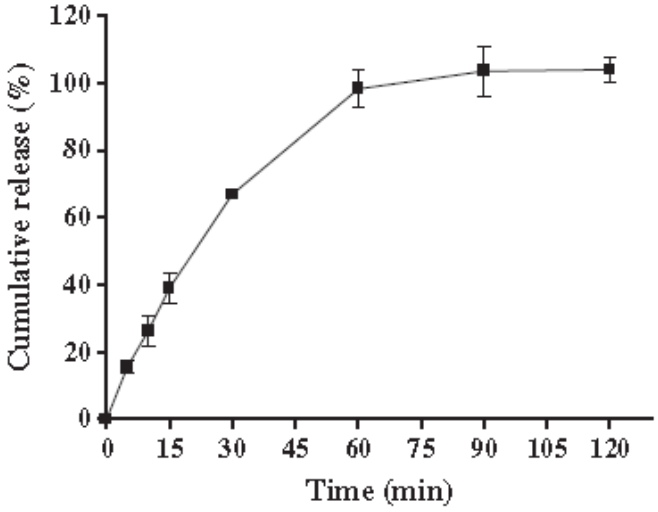

(Journal of Controlled Release, Fig.3)

Fig. 14. *In vitro* release profile of insulin from insulin-loaded MNs in pH 7.4 PBS maintained at 32 °C. Results are presented as the mean ± S.E. of 4 experiments.

2.2.6. *In vivo* transdermal absorption of insulin in diabetic rats

2.2.6.1. Methods

Rats were injected via the tail vein with 50 mg/kg of streptozotocin dissolved in citric acid buffer solution (pH 4.5) to produce a diabetic animal model. After approximately two weeks, rats with plasma glucose levels exceeding 300 mg/dl were deemed as diabetic. Prior to experimentation, diabetic rats were fasted for 14 h, while being provided water *ad libitum*. All animals were anesthetized via an intraperitoneal injection of 35mg/kg of pentobarbital sodium, and the abdominal region was carefully shaved. After the initial surgery and a 45 minute recovery period, plasma glucose and insulin baseline values were recorded. The following groups of diabetic animals were studied before and after drug administration: (1) MNs group, where 0.13, 0.25, and 0.44 IU insulin-loaded MNs were applied onto abdominal skin and fixed with tape; (2)MNs-pretreated group, where MNs without insulin were applied onto abdominal skin, removed 5 min later, and a piece of cotton saturated with insulin solution (5 IU/ml) was applied onto the MNs-pretreated area throughout the experiment; (3) subcutaneous group, where insulin solution (5 IU/ml, 50 μl) was injected subcutaneously into abdominal skin using a hypodermic needle and syringe; and (4) control group, where similar to the MNs groups, MNs without any insulin were applied onto abdominal skin. In all groups, blood samples were collected from jugular vein at 0, 0.5, 1, 2, 3, 5 and 7 h after the administration and centrifuged at 10,000 rpm for 5 min to immediately separate the plasma. Plasma glucose levels were determined via a glucose CII-Test kit, where the initial levels were considered as 100%. Using the initial values, the percent change in plasma glucose levels at each time interval after dosing was calculated. Plasma insulin concentrations were measured via an insulin-EIA Test kit.

The minimum glucose level (C_{min}) and the time point of minimum glucose level (T_{min}) were determined from profiles generated by plotting the percent change from initial levels of plasma glucose against time. The area above the curves (AAC) for 0–7 h was calculated using the trapezoidal method. The relative pharmacological availability (RPA) was calculated according to the following equation:

$$RPA(\%) = (AAC_{MN} \times Dose_{S.C.})/(AAC_{S.C.} \times Dose_{MN}) \times 100$$

Where AAC_{MN} shows the area above the curves after applying theinsulin-loaded MNs, and $AAC_{S.C.}$ indicates the area above the curves after subcutaneous injection of insulin.

The maximum plasma insulin concentration (C_{max}) and the timepoint of maximum plasma insulin concentration (T_{max}) were determinedfrom profiles generated by plotting the plasma insulin concentration(μIU/ml) versus time. The area under the curves (AUC) for 0–7 hwas calculated according to the trapezoidal method. Additionally, relativebioavailability (RBA) was calculated from the following equation:

$$RBA(\%) = (AUC_{MN} \times Dose_{S.C.})/(AUC_{S.C.} \times Dose_{MN}) \times 100$$

Where AUC_{MN} shows the area under the curves after applying theinsulin-loaded MNs, and $AUC_{S.C.}$indicates the area under the curvesafter subcutaneous injection of insulin.

All statistical analyses were performed using GraphPad Prism software (GraphPad Software Inc., San Diego, CA, USA). Descriptive statistics are presented as mean ± SE. A Student's paired t-test was used for comparisons between data points. Multiple data sets between groups were analyzed with a one-way analysis of variance (ANOVA) followed by a Tukey's post hoc test, when appropriate. Multiple data sets within groups were analyzed with an ANOVA followed by a Dunnett's post hoc test, when appropriate. For all comparisons, $p<0.05$ was considered to be statistically significant.

2.2.6.2. Results and Discussion

Diabetes was successfully induced in rats two weeks after an injection of streptozotocin, as they displayed a pronounced hyperglycemia (437.0 ± 11.5 mg/dl). The effects of various doses of insulin on changes in plasma glucose levels of diabetic rats after treatment with insulin-loaded MNs are presented in Fig.15A. A significant and dose-dependent

hypoglycemic effect was observed after treatment with insulin-loaded MNs of varying doses in comparison to the control ($p<0.0001$) The maximum percent decrease from baseline in plasma glucose levels ranged from 11.9% to 57.4% when insulin doses of 0.13-0.44 IU were administered via MNs. These findings suggest that the extent of the hypoglycemic response can be easily controlled by varying the amount of insulin loaded in the novel MNs. Plasma insulin concentrations following the treatment of diabetic rats with insulin-loaded MNs were also directly measured. It was found that, in comparison to the control, there was a significant and dose-dependent increase in plasma insulin concentrations after treatment with insulin-loaded MNs (Fig. 15B). The peak plasma levels of insulin were obtained within an hour and ranged from 62.6–151.4 μIU/ml, when insulin doses of 0.13–0.44 IU were administered via MNs ($p<0.01$).These findings suggest that insulin is being absorbed from the MNs via the skin, and that the novel MNs system is effective in the transdermal delivery of insulin.

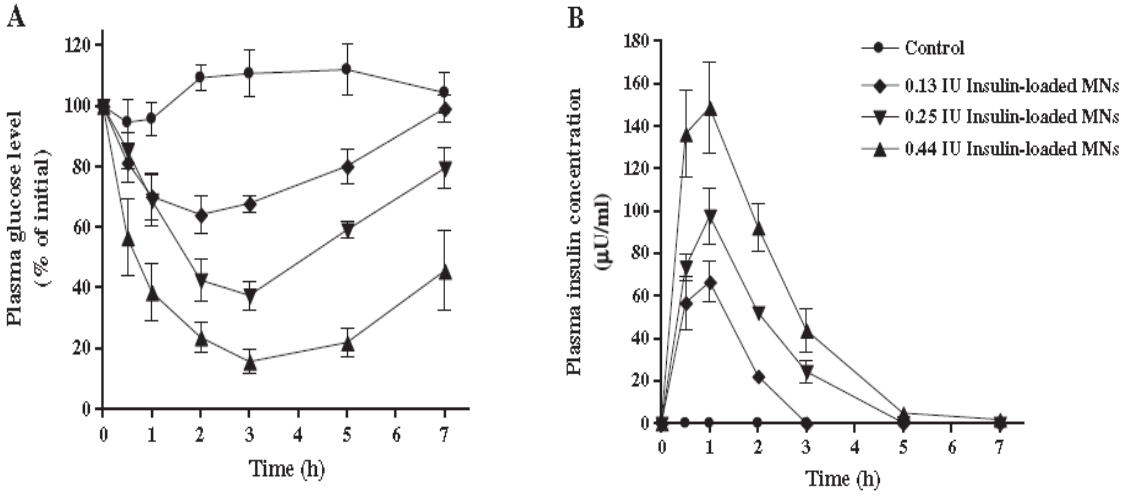

(Journal of Controlled Release, Fig.6)

Fig. 15.Effects of insulin dose on the percentage change in (A) plasma glucose levels and (B) plasma insulin concentrations in diabetic rats after an administration of 0.13-0.44 IU insulin-loaded MNs. Results are presented as the mean ± S.E. of 6 experiments.

The effects of various application methods of insulin on the changes in plasma glucose levels in diabetic rats are presented in Fig. 16A. A rapid decrease in plasma glucose levels was seen after a subcutaneous injection of 0.25 IU of insulin, and the maximum decrease in plasma glucose levels was approximately 40 % of its initial value. A similar hypoglycemic effect was found after treatment with insulin-loaded MNs at the same dose of insulin as that of the subcutaneous injection group. However, the onset of hypoglycemic response and peak plasma insulin levels was slightly slower with the MNs than the subcutaneous injection. These findings corroborate the results of Ito et al., who used insulin-loaded MN fabricated from dextrin and mixed with insulin, and demonstrated a slower onset time, but a more stable hypoglycemic effect in the case of the insulin-loaded MNs, as compared with the subcutaneous injection [26]. The gradual release of insulin can be attributed to the time necessary for the insulin-loaded MNs to dissolve versus the rapid delivery of insulin by a subcutaneous injection, as confirmed in the measurement of plasma insulin concentrations. In contrast to MNs, there were no significant changes in plasma glucose levels in the MNs-pretreated group compared with the control group over the 7-hour period. Plasma insulin levels of diabetic rats after insulin administration via various methods are presented in Fig. 16B. Treatment with insulin-loaded MNs resulted in lower peak plasma levels, but higher plasma insulin concentrations after 2 h, than those of the subcutaneous group. Conversely, in the MNs-pretreated group, there was a small spike in plasma insulin concentrations compared to those achieved with insulin-loaded MNs and a subcutaneous injection of insulin. Therefore, insulin could not be delivered across the MNs pretreated skin into the systemic circulation, despite the application of an insulin solution to the skin. In previous studies, transdermal drug delivery was shown to be dramatically increased after pre-treating skin with insoluble MNs prior to drug administration [18, 19, 65, 66]. The reasons for this discrepancy are unknown, but may be related to several factors. First, the novel HA MNs easily dissolve in skin, and therefore, the diffusion of insulin via the pores created by the HA MNs may be interfered due

to the presence of MNs components. Furthermore, the concentration of insulin solution used in the study may have been too low to obtain the therapeutic efficacy seen in previous studies, which used higher concentrations of insulin solutions (100-500 U/ml) to achieve hypoglycemic effects in diabetic rats [17, 65, 66, 68, 69]. However, it should be mentioned that similar concentrations of insulin (5 U/ml) were used in order to properly evaluate the effects of the application method used in insulin delivery. Additionally, Zhou et al. and Wu et al. reported that a large amount of insulin penetrates through the skin after the application of high concentrations of insulin at the donor site [18, 19]. Therefore, almost no significant pharmacological effect of applying a low concentration of insulin solution was found in this study. Furthermore, it may be plausible that the pores created by MNs were reversible, as confirmed by the TEWL measurements, and thereby the diffusion of insulin gradually reduced with time after the removal of MNs. Therefore, these factors may be associated with the null results obtained in the MNs-pretreated group; however, further studies that clarify the exact mechanisms responsible for these findings are warranted.

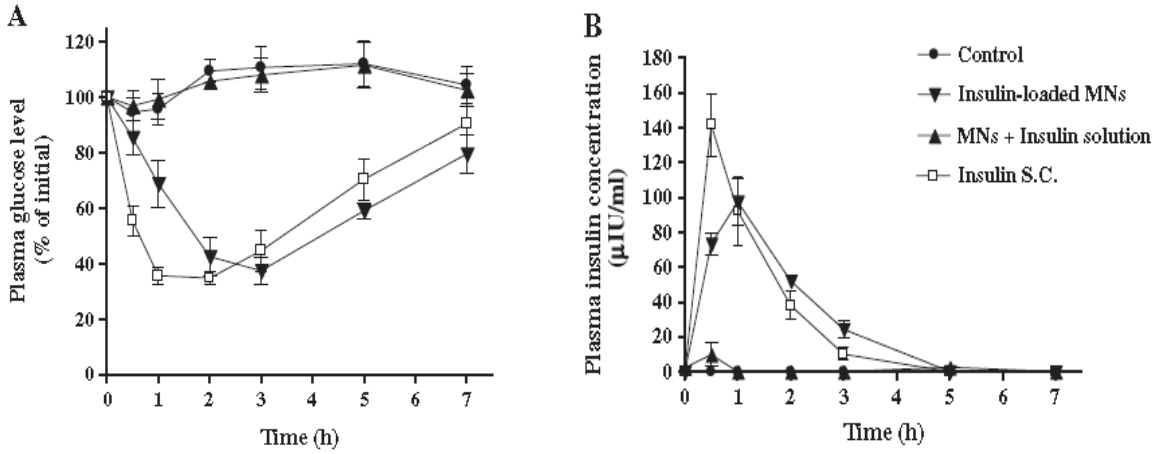

(Journal of Controlled Release, Fig.7)

Fig. 16.Effects of various application methods of insulin on (A) plasma glucose levels and (B) plasma insulin concentrations in diabetic rats. Results are presented as the mean ± S.E. of 6 experiments.

The pharmacodynamic parameters of plasma glucose levels and pharmacokinetic parameters for plasma insulin concentrations were calculated and presented in Tables 3 and 4, respectively. As evident from Table 3, the RPA of insulin after treatment with insulin-loaded MNs of varying doses ranged from 93.6 % to 97.9 %. Similarly, as evident from Table 4, RBA of insulin after treatment with insulin-loaded MNs of varying doses ranged from 96.1 % to 98.8 %. It demonstrates that insulin could be completely delivered into the systemic circulation using insulin-loaded MNs fabricated of HA. A comparable hypoglycemic effect and insulin delivery were achieved with insulin loaded MNs and the subcutaneous injection. These MNs were equally effective to subcutaneous injection. These findings suggest that the novel HA MNs are excellent candidates for delivering insulin to diabetic patients. Moreover, a very small RPA (i.e., 2.34 %) and RBA (i.e., 5.32 %) of insulin solution indicates that a marginal hypoglycemic effect and insulin delivery were achieved with the application of an insulin solution to MNs-pretreated skin. Additionally, MRT of insulin-loaded MNs of varying dose ranged from 1.3 h to 1.6 h without significant difference among them. The possible increasing trend may be caused by the interaction of insulin and hyaluronic acid which impacts the release and absorption of insulin from MNs.

Table 3 Pharmacodynamic parameters for the plasma glucose levels of diabetic rats after an administration of insulin-loaded MNs, a subcutaneous injection of insulin (insulin S.C.), and an insulin solution after pretreatment with MNs (MNs+insulin solution).

Group	**C_{min} (%)**	**T_{min} (hr)**	**AAC 0→7 (% hr)**	**RPA (%)**
Control	88.8 ± 4.1	0.5 ± 0.2	15.9 ± 7.0	–
0.13 IU insulin-loaded MNs	57.4 ± 6.7	2.0 ± 0.3	144.6 ± 21.5***	97.9 ± 15.4
0.25 IU insulin-loaded MNs	30.1 ± 3.3	2.7 ± 0.2	285.3 ± 15.9***	97.5 ± 5.4
0.44 IU insulin-loaded MNs	11.9 ± 3.0	3.7 ± 0.6	481.8 ± 25.7***	93.6 ± 5.0
0.25 IU insulin S.C.	28.2 ± 1.2	1.5 ± 0.3	292.5 ± 24.1***	100
MNs + 0.25 IU insulin solution	92.3 ± 4.2	0.5 ± 0.2	6.9 ± 4.0	2.3 ± 1.4

Results are presented as the mean ± S.E. of at least 6 experiments. $^{***}p<0.001$, compared with the control. (Journal of Controlled Release, Table 2)

Table 4 Pharmacokinetic parameters for plasma insulin concentrations of diabetic rats after administration of insulin-loaded MNs, subcutaneous injection of insulin (insulin S.C.) and insulin solution after pretreatment by MNs (MNs+insulin solution).

Group	C_{max} (μIU/ml)	T_{max} (h)	$AUC_{0\rightarrow7}$ (μIU h/ml)	RBA (%)	MRT （h）
Control	0	0	0	0	0
0.13 IU insulin-loaded MNs	62.6 ± 12.4	1.0 ± 0.0	100.6 ± 13.1***	96.1 ± 12.5	1.3 ± 0.1
0.25 IU insulin-loaded MNs	98.9 ± 12.7	0.7 ± 0.1	198.8 ± 15.6***	98.8 ± 7.7	1.5 ± 0.1
0.44 IU insulin-loaded MNs	151.4 ± 27.2	0.7 ± 0.2	348.8 ± 38.7***	98.5 ± 10.9	1.6 ± 0.2
0.25 IU insulin S.C.	155.4 ± 13.7	0.6 ± 0.1	201.3 ± 16.2***	100	1.2 ± 0.1
MNs+0.25 IU insulin solution	9.9 ± 6.7	0.3 ± 0.1	10.7 ± 6.8	5.3 ± 3.7	0.3 ± 0.1

Results are presented as the mean ± S.E. of at least 6 experiments. *** $p< 0.001$, compared with the control. (Journal of Controlled Release, Table 3)

2.3 Application in the transdermal delivery of exendin-4 using tip-loaded MNs

2.3.1. Determination of drug contents in tip-loaded microneedle arrays

2.3.1.1. Methods

In this study, we prepared FD4 tip-loaded MNs with doses of 1, 2 and 4 μg FD4/microneedle array. For determination of FD4 contents in the tip-loaded MNs, needles on arrays were collected and dissolved in pH 7.4 PBS followed by 30 min of sonication. FD4 was analyzed using a fluorescence HPLC system (Hitachi, Kyoto, Japan). Samples were eluted on a C18 column (5C18-AR- II, 4.6x150 mm; Nacalai Tesque, Kyoto, Japan) using a mobile phase consisting of 0.1% phosphoric acid and acetonitrile (80:20). A flow rate of 1 ml/min was maintained. The excitation wavelength was 485 nm and the emission wavelength was 585 nm.

2.3.1.2. Results and Discussion

As shown in Fig. 17, the drug was designed to be loaded into tips (yellow part) of MNs with a length of about 200 μm. Each needle was approximately 800 μm in height, with a

diameter of 160 μm at the base and 40 μm at the tip, and an interspacing of 600 μm between the rows of needles. There were approximately 140 needles in a circular area with a diameter of 10 mm. Although Sullivian et al. have reported microneedles with model drug located only in part of needles [70], the model drug in the tip-loaded MNs in the study is more concentrated to the top 1/4 of needles compared with their needles. Moreover, there is clear border line between the part with drug loaded and the part without drug loaded as shown in Fig.17.

FD4 was used as a model drug loaded into the tips of MNs in order to evaluate tip-loaded drug dose and reproducibility. The experimentally measured contents of FD4 in the tip-loaded MNs were determined and are summarized in Table 5. As shown in Table 5, the amount of FD4 loaded in MNs was found to be largely coincided with the calculated dose, although there was a very small standard error, particularly in the case of exendin-4 administration at low dose.

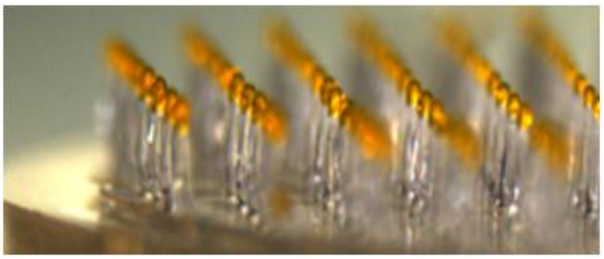

Fig.17. FD4 tip-loaded MNs observed by a microscope

Table 5 FD4 content of FD4 tip-loaded MNs

Dose of FD4 (μg/patch)	Content (% of dose)
1	106.58 ± 8.90
2	102.43± 4.70
4	99.12± 5.68

Results are presented as means ± S.E. of 4 experiments in each group.

2.3.2. *In vitro* release study

2.3.2.1. Methods

Release of FD4 from the tip-loaded MNs across Silescol® membranes was investigated using *in vitro* modified Franz cells. The content of FD4 in tip-loaded MNs was 4 μg/microneedle array. After application of MNs, the membranes with tip-loaded MNs were mounted onto Franz cells. Cells were positioned upright and receptor compartments were filled with 2.4 ml of pH 7.4 PBS maintained at 32°C throughout the test period. At pre-determined intervals, 0.2 ml of supernatant was withdrawn and replaced with an equal volume of fresh release medium. FD4 was analyzed by fluorescence HPLC as described above.

2.3.2.2. Results and Discussion

The cumulative release of FD4 from tip-loaded MNs was determined via an *in vitro* release study (Fig. 18). FD4 tip-loaded MNs were readily dissolved and FD4was rapidly released from the MNs, particularly in the initial 30 s after the start of the experiment. In the present study, most FD4 was released within 5 min, suggesting that the release of FD4 was very rapid from its tip-loaded MNs. These rapid release profiles for FD4 are superior when compared with dissolving MNs. For instance, the time needed for contained drug release varies from 25 min in galactose MNs [29] to 120 h in amylopectin MNs [27].Moreover, insulin was released within 1 h from the HA MNs containing insulin in our previous study. As compared with our previous MNs, it is clear that the drug release time can be shortened by drug tip-loading.

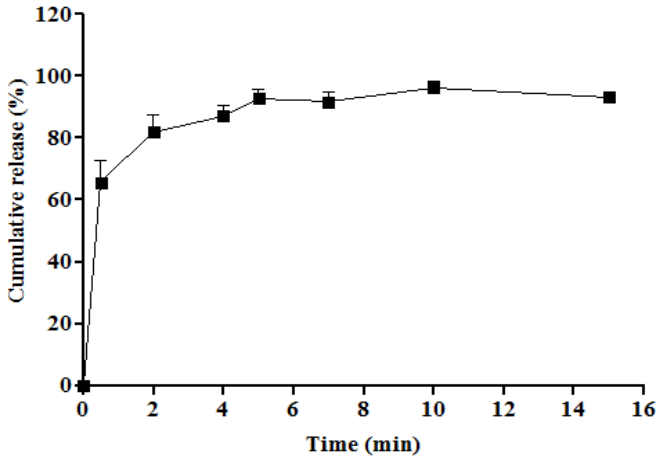

Fig.18 *In vitro* release of FD4 from FD4 tip-loaded MNs in pH7.4 PBS maintained at 32°C.Results are expressed as means ± S.E. of 4 experiments.

2.3.3. Acute efficacy in IPGTTs

2.3.3.1. Methods

The acute efficacy of exendin-4 tip-loaded MNs was evaluated by IPGTTs in type 2 diabetic GK/Slc rats after application of MNs, as compared with subcutaneous injection. GK/Slc rats were fasted for 14 h and anesthetized by intraperitoneal injection of 35mg/kg pentobarbital sodium, and their abdominal regions were carefully shaved. After initial surgery and a 1 h recovery period, GK/Slc rats were randomly allocated into five groups and then treated as follows:

(a) Transdermal application of exendin-4 tip-loaded MNs containing 10 μg/kg exendin-4

(b) Transdermal application of exendin-4 tip-loaded MNs containing 50 μg/kg exendin-4

(c) Subcutaneous injection of 10 μg/kg dose of exendin-4 solution

(d) Subcutaneous injection of 50 μg/kg dose of exendin-4 solution

(e) Transdermal application of MNs without exendin-4

Thirty minutes after administration of exendin-4 in each group, glucose (dose; 2g/kg) was then intraperitoneally administered to each rat. At predetermined times, blood samples were collected from the jugular vein and were centrifuged at 10,000 rpm for 5 min in order to

separate plasma immediately. Plasma glucose levels were determined using a glucose CII-Test kit and plasma glucose levels at 0 min were considered to be 100%. Using this value, the percentage change in plasma glucose levels at each time point after dosing was calculated. Plasma concentrations of endogenous insulin were measured using a rat insulin ELISA kit, and plasma concentrations of exendin-4 were determined using exendin-4 EIA kit. All statistical analyses were performed as mentioned above in 2.2.6.1.

2.3.3.2. Results and Discussion

In order to compare the efficacy of exendin-4 tip-loaded MNs with traditional subcutaneous injection, glucose tolerance, insulin secretion and plasma concentrations of exendin-4 were examined in IPGTTs in type 2 diabetic GK/Slc rats *in vivo*. The experimental conditions were designed according to the method of Arakawa et al. [71] and administration of exendin-4 was conducted 30 min before glucose challenge for better observation of insulin secretion in response to glucose change. Fig. 19 compares exendin-4 tip-loaded MNs and subcutaneous injection of exendin-4 on glucose tolerance in IPGTTs. As shown in Fig. 19A, blood glucose levels in the control group rapidly increased and reached a maximum value of 235.47 ± 10.91% of initial levels at 30 min after intraperitoneal glucose challenge. Dose-dependent suppression of the increased blood glucose levels was observed after subcutaneous pre-administration of 10 μg/kg and 50 μg/kg exendin-4 when compared with the control group, and blood glucose values at 30 min in subcutaneous injection of 10 μg/kg and 50 μg/kg exendin-4 groups after intraperitoneal glucose challenge were 188.63 ± 9.14 % and 126.57 ± 17.73 %, respectively. In the case of the exendin-4 tip-loaded MN group, normalization effects on blood glucose were found to be similar to the subcutaneous injection groups and blood glucose values at 30 min in 10 μg/kg and 50 μg/kg exendin-4 tip-loaded MNs groups after intraperitoneal glucose challenge were 176.17 ± 13.35 % and 137.66 ± 2.91 %, respectively. Moreover, as shown in Fig. 19B, calculated glucose $AUC_{0\text{-}120\ min}$ values in both

of the MNs and the subcutaneous injection groups significantly decreased when compared with the control group. In addition, there were no significant differences in the calculated glucose $AUC_{0\text{-}120\ min}$ values between MN groups and subcutaneous injection groups after administration of exendin-4 at the same dose.

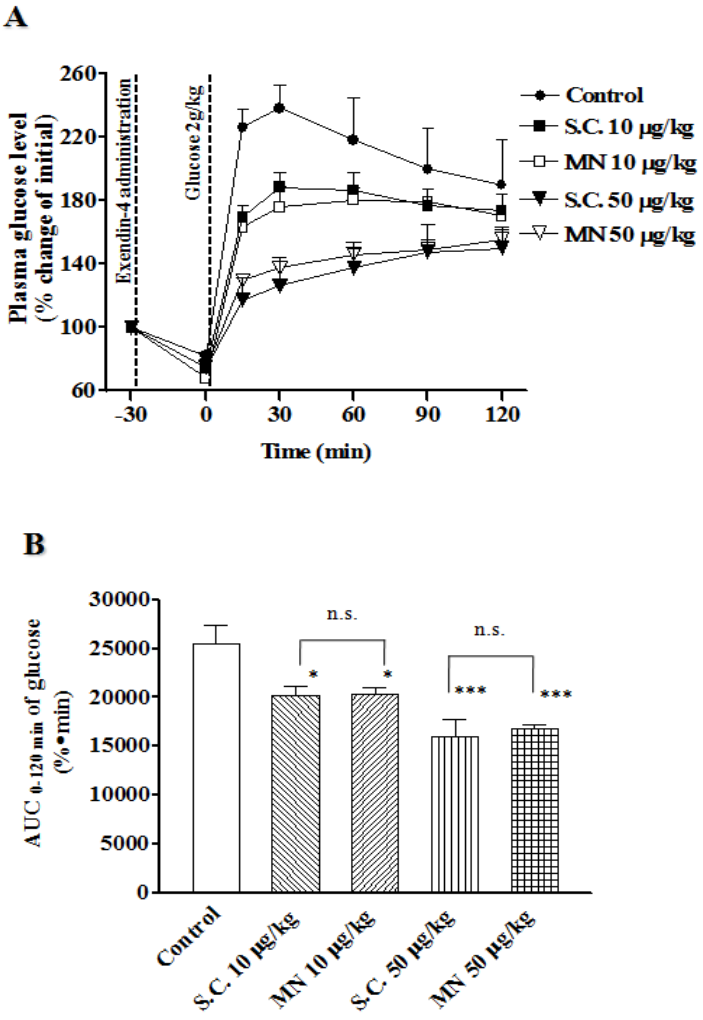

Fig. 19 Acute effects of administration of exendin-4 by subcutaneous injection (S.C.) and exendin-4 tip-loaded M.N. on glucose tolerance in GK rats (A), and calculated glucose $AUC_{0\text{-}120\ min}$ (B). Intraperitoneal glucose tolerance tests (IPGTTs) were carried out 30 min after administration of exendin-4 (S.C. and M.N.). Results are presented as means ±S.E. of at least 5 experiments in each group. (***) $p< 0.001$ and (*) $p< 0.05$, compared with controls.

Fig. 20 shows plasma insulin levels in the control group, exendin-4 tip-loaded MN group

and subcutaneous injection group in IPGTTs. The stimulation of insulin secretion by exendin-4 appeared to be dependent on glucose levels in both of MNs and SC groups. This behavior is similar to previous studies, in which acute administration of exendin-4 lowered the glycemic response to glucose challenge as a result of augmented insulin secretion [71]. In the control group, insulin secretion increased slightly after intraperitoneal glucose challenge with a C_{max} value of 1.89 ± 0.32 ng/ml at 15 min. In contrast, insulin secretion was markedly increased by subcutaneous injection of 10 μg/kg and 50 μg/kg exendin-4. The C_{max} value in the case of 10 μg/kg subcutaneous injection of exendin-4 was3.10 ± 0.56 ng/ml, while 50 μg/kgsubcutaneous injection of exendin-4 had a C_{max} value of 4.83 ±0.32 ng/ml. On the other hand, similar results were observed on insulin secretion in the exendin-4 tip-loaded MN groups. C_{max} values of 10 μg/kg and 50 μg/kgexendin-4 tip-loaded MN groups were 3.13 ± 0.24 ng/ml and 4.45 ± 0.48 ng/ml, respectively. The glucose normalization effects lasted longer than stimulation of insulin secretion, which is consistent with a previous report by Arakawa et al [71].It is possible that the insulin response was blunted, even though glucose was at much higher basal levels after rapid release during the initial phase (0-10 min), as shown in the pancreas perfusion study in GK rats by Edholm et al.[72] In addition, as shown in Fig. 20 B, calculated insulin $AUC_{0\text{-}60\ min}$ values in both the exendin-4 tip-loaded MN and subcutaneous injection groups significantly increased when compared with controls. A dose-dependent increase in insulin $AUC_{0\text{-}60\ min}$ values was observed in MNs and subcutaneous groups, and there were no significant differences in insulin secretion between exendin-4 tip-loaded MNs group and the subcutaneous injection group.

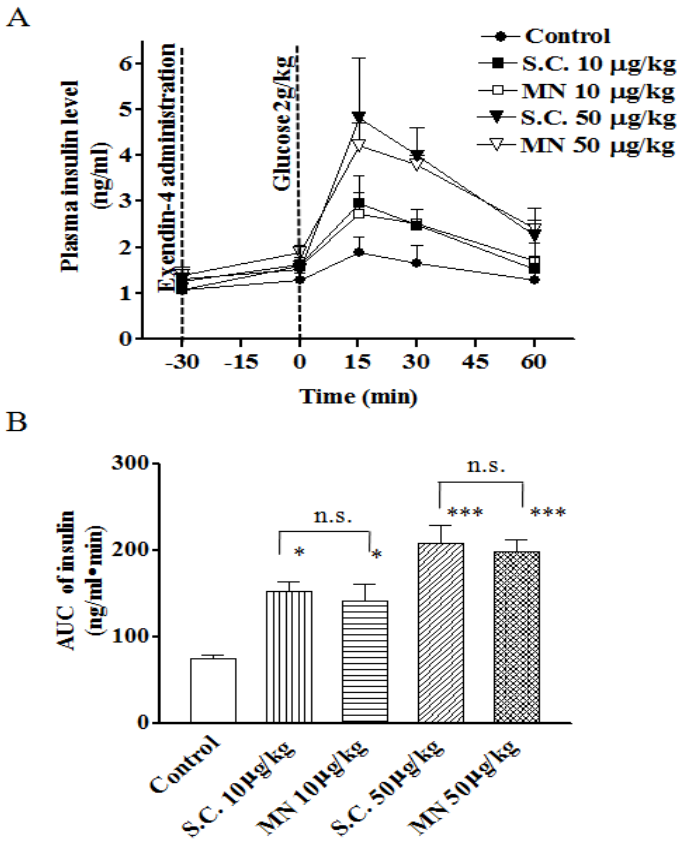

Fig. 20 Acute effects of exendin-4 (S.C. and M.N.) on plasma insulin response to glucose (2g/kg) in GK rats (A), and calculated insulin $AUC_{0\text{-}60\ min}$ (B). Intraperitoneal glucose tolerance tests (IPGTTs) were carried out at 30 min after administration of exendin-4 (S.C. and M.N.). Results are presented as means ±S.E. of at least 5 experiments in each group. (***) $p < 0.001$ and (*) $p < 0.05$, compared with controls

Fig. 21 shows plasma profiles of exendin-4 in GK rats after the application of exendin-4 tip-loaded MNs and subcutaneous injection in IPGTTs. In subcutaneous injection of exendin-4 groups, plasma concentrations of exendin-4 rapidly increased and peaked at C_{max} values of 19.86 ± 9.93ng/ml (10 μg/kg subcutaneous injection of exendin-4) and 66.70 ± 26.11ng/ml (50 μg/kg subcutaneous injection of exendin-4), respectively. The values decreased to baseline at 120 min after glucose challenge. In the case of exendin-4 tip-loaded MNs, the plasma concentration-time profiles of exendin-4 were closely correlated with subcutaneous injection of exendin-4 at the same dose. It also indicated that exendin-4 was

rapidly released from the tip-loaded MNs. As illustrated in Fig. 21B, the calculated $AUC_{-30\text{-}120min}$ values of exendin-4 were significantly higher in both the exendin-4 tip-loaded MNs group and the subcutaneous injection of exendin-4 group than in that of the control group. Moreover, a dose-dependent increase in $AUC_{-30\text{-}120min}$ values of exendin-4 was seen in the exendin-4 tip-loaded MN group. No significant differences were observed in $AUC_{-30\text{-}120min}$ values of exendin-4 between the exendin-4 tip-loaded MN group and the subcutaneous injection of exendin-4 group after application of the same dose of exendin-4. Taken together, these results suggest that the efficacy of exendin-4 tip-loaded MNs is almost equivalent to that after subcutaneous injection.

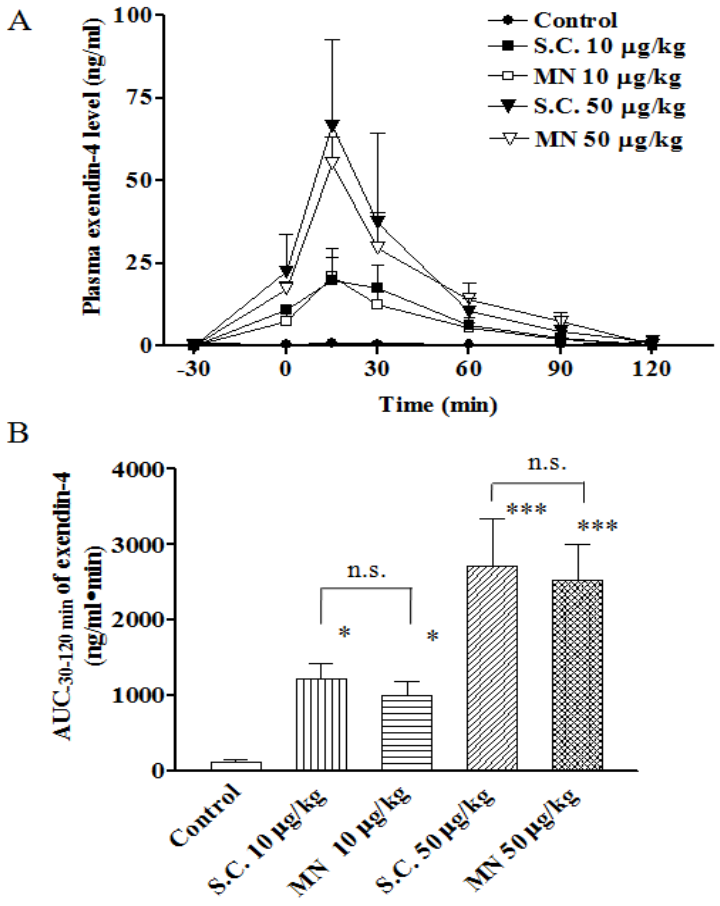

Fig. 21 Plasma concentration-time profiles of exendin-4 (S.C. and M.N.) in GK rats (A) and calculated exendin-4 $AUC_{-30\text{-}120\ min}$(B). Results are presented as means ±S.E. of at least 5 experiments in each group. (***) $p< 0.001$ and (*) $p< 0.05$, compared with controls.

DISCUSSION

In the present study, the novel MNs fabricated from hyaluronic acid is found to have several advantages over previous MNs. Firstly, as a major component of skin, hyaluronic acid is reasonably expected to overcome the safety issues when applied to silicon and metal MNs. Moreover, its high water soluble characteristic makes it easy and suitable for mass production, in contrast to other published methods that require more complex multistep fabrication schemes.

To overcome the risk of complications, other biocompatible and biodegradable MNs have been developed, such as the biodegradable polymers, including poly-lactide-*co*-glycolide acid, polylactic acid, polyglycolic acid and polycarbonate [24-26]. If left in the skin, these types of needles safely degrade and eventually disappear. They are also easy for production, but a heating step or organic solvent is mainly required for the casting. For that reason, although they also have the potential for loading drugs into a matrix of needles and releasing them in the skin by biodegradation in the interstitial fluid, they are not suitable to loading heat-sensitive drugs and peptides, such as insulin, and in turn, which eradicate their pharmacological activities. Superior to these MNs, the water soluble HA MNs simply load drugs within the needle matrix by molding the water solution of HA and drugs at room temperature, and thereby provide a simple one-step application process that is efficient in drug delivery. Moreover, the absence of organic solvents and elevated temperatures gives the HA MNs notable advantages for preserving peptide and biomolecule stability.

Most of the abovementioned biodegradable polymer needles have slow-degrading characteristics which can retain drugs in the skin for a long period of time. Therefore, they are not suitable for rapid delivery of drugs. Unlike these MNs, HA MNs are readily soluble and dissolve in skin within hours, and the release of drug is found able to further accelerate when loading drug in the tip part of needles. Besides the HA used in this study with the molecule

weight of 100,000 Da, there are many HA raw materials which range in size from 5,000 to 20,000,000 Da. By adjusting the composition of MN with these HA, the releasing profile of drug from HA MNs is considered able to be further modified for different clinical need from rapid drug delivery to sustained release without initial burst. In addition, in some prototyping, HA MNs is found able to load small particles such as the nanoparticles made of poly-lactide-*co*-glycolide acid, which indicates the possibility to further control the release of drug with the combination of some sustained release approaches.

Besides polymeric needles, the MNs made of carbohydrates, such as maltose [27-29] and galactoses [30], and dextrin [21, 31] was reported, which are readily soluble and dissolve in skin within minutes. However, in a wet environment exceeding humidity levels of 43% to 50%, these MNs are rapidly dissolved due to hydrolysis, which lead to a rapid deformation or disappearance of needles, and poor insertion ability into the skin [28, 30]. In contrast to these soluble MNs, the HA MNs have good water soluble property as well as suitable resistance to high humidity. The HA MNs are considered to be strong enough to reliably pierce into skin even in the wet environment with 75% humidity for 1 h which is long enough for MNs application. However, a sealed packaging is recommended to protect the MNs from wet environment till use.

The capacity limitation of drug in HA MNs depends on the physiccochemical properties of the drugs and their interaction with HA. Based on the experience in prototyping of the HA MNs containing alendronate, FD4, insulin and exendin-4, the capacity limitation is found able to be over 10 % which is equal to about 5 mg/cm^2 when the drug is loaded in whole MNs patch and 0.1 mg/cm^2 when the drug is loaded in needles. Namely, the insulin (28U/mg) loading in whole patch is able to be 140 U/cm^2 and the loading in needles is able to be 2.8 U/cm^2. It is known that initial insulin dose of usual adult dose for diabetes Type 1 is 0.5-0.8U/kg/day subcutaneously (a total daily insulin requirement is about 35-56U/human if the body weight is 70kg). To achieve such insulin administration, the total daily application

area of the abovementioned 140 U/cm^2 and 2.8 U/cm^2 insulin loading MNs is 0.25-0.4 cm^2 and 12.5-20 cm^2 by calculation, respectively. In both cases, their total daily application area is practical for clinical use, indicating the potential of HA MNs for insulin administration. Therapeutic dose of exendin-4 (Byetta) for diabetes Type 2 is twice-daily injection of 5-10 μg/human (a total weekly dose is 70-140 μg/human). Therefore, HA MNs can even provide sufficient dose for sustained release of exendin-4 with reasonable application area.

In this study, the drug is uniformly mixed with the main material of HA in the matrix of MNs for rapid drug delivery, and the drug release from HA MNs is observed to be within 1 hour. Therefore, an initial burst wasn't observed in the *in vitro* release study. However, it needs to be evaluated in the development to avoid hypoglycemia especially in case of sustained release of insulin. For successful MNs application, one suggestion is to use an applicator to well control the energy applied on MNs and provide consistent insertion in skin because the insertion depth and the insertion ratio of the HA MNs may vary due to application force and skin property of different subjects. The other suggestion is to apply MNs within 1 h after taking out from the sealed package although the HA MNs have good resistance to moisture compared with previous soluble MNs.

CONCLUSION

Chapter 1:

1) The novel self-dissolving MNs from HA were able to uniformly puncture the skin without breakage and release drug to the dermis along with the dissolution in skin.
2) The skin disruption caused by HA MNs was reversible, and the pore created by MNs was observed to almost recover at 24 h after application. These findings from TEWL and TER measurements and *in vivo* dermatosope observation indicated the safety of MNs which is further confirmed by a skin primary irritation test.
3) The HA MNs containing FD4 were found to be much more effective for increasing the amount of permeation and tissue accumulation in the skin as compared with the solution formulation.

Chapter 2:

1) The insulin-loaded HA MNs possessed suitable hygroscopy, stability and drug releasing profiles. Insulin administered via MNs was almost completely absorbed from the skin into the systemic circulation without any serious damage to skin in diabetic rats.
2) The exendin-4 tip-loaded MNs provided rapid exendin-4 administration. They showed comparable acute effects on glucose tolerance, insulin secretion and plasma concentration profiles, as compared with subcutaneous injection, in type 2 diabetic GK/Slc rats.

To sum up, HA MNs are a useful alternative method to improve the transdermal delivery of drugs, especially drug with relatively high molecular weight without seriously damaging the skin. They might be effective and safe dosage form for transdermal delivery in the clinical setting.

ACKNOWLEDGMENTS

I wish to express my sincere gratitude to:

Professor Akira Yamamoto, my academic supervisor, for his guidance, patience and genuine enthusiasm throughout my academic years;

Associate Professor Toshiyasu Sakane, Dr. Hidemasa Katsumi, Dr. Fumio Kamiyama and Dr. Ying-shu Quan, for providing good work facilities, their kind guidance and valuable suggestions in this research;

Dr. Ying-zhe Li, Dr. Zheng-qi Dong, Ms. Mei-na Jin, Ms Dan Wu and all members of the Department of Biopharmaceutics, for their kind supports, collaboration and friendly assistance;

Last, but not least, my husband, parents, family and friends, for their understanding, constant support and boundless love throughout my academic years.

REFERENCES

[1] Y.C. Kim, J.H. Park, M.R. Prausnitz. Microneedles for drug and vaccine delivery. Adv. Drug Deliv. Rev. 64 (2012) 1547-1568.

[2] V. Sachdeva, A.K. Banga. Microneedles and their applications. Recent Pat. Drug Deliv.Formul. 5 (2011) 95-132.

[3] D.V. McAllister, P.M. Wang, S.P. Davis, J.H. Park, P.J. Canatella, M.G. Allen, M.R. Prausnitz, Microfabricated needles for transdermal delivery of macromolecules and nanoparticles: fabrication methods and transport studies. Proc. Natl. Acad. Sci. U.S.A. 100 (2003) 13755–13760.

[4] R.K. Sivamani, B. Stoeber, G.C. Wu, H. Zhai, D. Liepmann, H. Maibach, Clinical microneedle injection of methyl nicotinate: stratum corneum penetration. Skin Res. Technol. 11 (2005) 152–156.

[5] W. Martanto, J.S. Moore, O. Kashlan, R. Kamath, P.M. Wang, J.M. O'Neal, M.R. Prausnitz, Microinfusion using hollow microneedles. Pharm. Res. 23 (2006) 104–113.

[6] S.A. Coulman, A. Anstey, C. Gateley, A. Morrissey, P. McLoughlin, C. Allender, J.C. Birchall, Microneedle mediated delivery of nanoparticles into human skin. Int. J. Pharm. (2009) 190–200.

[7] S. Chandrasekaran, J.D. Brazzle, A.B. Frazier, Surface micromachined metallic microneedles. J. Microelectromech. Syst. 12 (2003) 281–288.

[8] S. Kaushik, A.H. Hord, D. Denson, D.V. McAllister, S. Smitra, M.G. Allen, M.R. Prausnitz, Lack of pain associated with microfabricatedmicroneedles.Anesth. Analg. 92 (2001) 502–504.

[9] H.S. Gill, D.D. Denson, B.A. Burris, M.R. Prausnitz, Effect of microneedle design on pain in human volunteers.Clin. J. Pain 24 (2008) 585–594.

[10] M.L. Reed, W.K. Lye, Microsystems for drug and gene delivery. Proc. IEEE 92 (2004)

56–75.

[11] Y. Xie, B. Xu, Y. Gao, Controlled transdermal delivery of model drug compounds by MEMS microneedle array.Nanomedicine 1 (2005) 184–190.

[12] R.F. Donnelly, D.I.J. Morrow, P.A. McCarron, A.D. Woolfson, A. Morrissey, P. Juzenas, A. Juzeniene, V. Iani, H.O. McCarthy, J. Moan, Microneedle-mediated intradermal delivery of 5-aminolevulinic acid: Potential for enhanced topical photodynamic therapy. J. Control. Release 129 (2008) 154–162.

[13] G. Yan, K.S. Warner, J. Zhang, S. Sharma, B.K. Gale, Evaluation needle length and density of microneedle arrays in the pretreatment of skin for transdermal drug delivery. Int. J. Pharm. 391 (2010) 7–12.

[14] S.L. Banks, R.R. Pinninti, H.S. Gill, P.A. Crooks, M.R. Prausnitz, A.L. Stinchcomb, Flux across microneedle-treated skin is increased by increasing charge of naltrexone and naltrexol*in vitro*. Pharm. Res. 25 (2008) 1677–1685.

[15] H. Chen, H. Zhu, J. Zheng, D. Mou, J. Wan, J. Zhang, T. Shi, Y. Zhao, H. Xu, X. Yang, Iontophoresis-driven penetration of nanovesicles through microneedleinduced skin microchannels for enhancing transdermal delivery of insulin. J. Control. Release 139 (2009) 63–72.

[16] A.J. Harvey, S.A. Kaestner, D.E. Sutter, N.G. Harvey, J.A. Mikszta, R.J. Pettis, Microneedle-based intradermal delivery enables rapid lymphatic uptake and distribution of protein drugs. Pharm. Res. 28 (2011) 107–116.

[17] P.M. Wang, M. Cornwell, J. Hill, M.R. Prausnitz, Precise microinjection into skin using hollow microneedles. J. Invest. Dermatol. 126 (2006) 1080–1087.

[18] Y. Wu, Y. Gao, G. Qin, S. Zhang, Y. Qiu, F. Li, B. Xu, Sustained release of insulin through skin by intradermal microdelivery system. Biomed. Microdev. 12 (2010) 665–671.

[19] C.P. Zhou, Y.L. Liu, H.L. Wang, P.X. Zhang, J.L. Zhang, Transdermal delivery of insulin

using microneedle rollers *in vivo*. Int. J. Pharm. 392 (2010) 127–133.

[20] X. Chen, T.W. Prow, M.L. Crichton, D.W.K. Jenkins, M.S. Roberts, I.H. Frazer, G.J.P. Fernando, M.A.F. Kendall, Dry-coated microprojection array patches for targeted delivery of immunotherapeutics to the skin. J. Control. Release 139 (2009) 212–220.

[21] H.S. Gill, M.R. Prausnitz, Coating formulations for microneedles. Pharm. Res. 24 (2007) 1369–1380.

[22] H.S. Gill, M.R. Prausnitz, Coated microneedles for transdermal delivery. J. Control. Release 117 (2007) 227–237.

[23] J.H. Park, M.G. Allen, M.R. Prausnitz, Polymer microneedles for controlled release drug delivery. Pharm. Res. 23 (2006) 1008–1019.

[24] C.Y. Jin, M.H. Han, S.S. Lee, Y.H. Choi, Mass producible and biocompatible microneedle patch and functional verification of its usefulness for transdermal drug delivery. Biomed. Microdev. 11 (2009) 1195–1203.

[25] R.F. Donnelly, R. Majithiya, T.R.R. Singh, D.I.J. Morrow, M.J. Garland, Y.K. Demir, K. Migalska, E. Ryan, D. Gillen, C.J. Scott, A.D. Woolfson, Design, optimization and characterization of polymeric microneedle arrays prepared by a novel laser-based micromoulding technique. Pharm. Res. 28 (2011) 41–57.

[26] Y. Ito, E. Hagiwara, A. Saeki, N. Sugioka, K. Takada, Feasibility of microneedles for percutaneous absorption of insulin. Eur. J. Pharm. Sci. 29 (2006) 82–88.

[27] J.W. Lee, J.H. Park, M.R. Prausnitz, Dissolving microneedles for transdermal drug delivery. Biomaterials 29 (2008) 2113–2124.

[28] G. Li, A. Badkar, S. Nema, C.S. Kolli, A.K. Banga, *In vitro* transdermal delivery of therapeutic antibodies using maltose microneedles. Int. J. Pharm. 368 (2008) 109–115.

[29] R.F. Donnelly, D.I.J. Morrow, R. Majithiya, T.R.R. Singh, K. Migalska, P.A. McCarron, C. O'Mahony, A.D. Woolfson, Processing difficulties and instability of carbohydrate microneedle arrays. Drug Dev. Ind. Pharm. 35 (2009) 1242–1254.

[30] Y. Ito, H. Murano, N. Hamasaki, K. Fukushima, K. Takada, Incidence of low bioavailability of leuprolide acetate after percutaneous administration to rats by dissolving microneedles. Int. J. Pharm. 407 (2011) 126–131.

[31] J.H. Oh, H.H. Park, K.Y. Do, M. Han, D.H. Hyun, C.G. Kim, C.H. Kim, S.S. Lee, S.J. Hwang, S.C. Shin, C.W. Cho, Influence of the delivery systems using a microneedle array on the permeation of a hydrophilic molecule, calcein. Eur. J. Pharm. Biopharm. 69 (2008) 1040–1045.

[32] J.H. Park, M.G. Allen, M.R. Prausnitza, Biodegradable polymer microneedles: fabrication, mechanics and transdermal drug delivery. J. Control. Release 104 (2005) 51–66.

[33] M. Takaya, T. Yoshikazu, K. Takahiro, M. Yasushi, T. Hitoshi, W. Makoto, H. Katsumi, Sugar micro needles as transdermic drug delivery system. Biomed. Microdevices 7 (2005) 185–188.

[34] V. Lassmann-Vague, D. Raccah. Alternatives routes of insulin delivery. Diabetes Metab. 32 (2006) 513-522.

[35] V.H.L. Lee, A. Yamamoto. Penetration and enzymatic barriers to peptide and protein absorption. Adv. Drug Deliv. Rev. 4 (1990) 171-207.

[36] A. Yamamoto, T. Fujita, S. Muranishi. Pulmonary absorption enhancement of peptides by absorption enhancers and protease inhibitors. J. Control. Release 41 (1996) 57-67.

[37] L. He, Y. Gao, Y. Lin, H. Katsumi, T. Fujita, A. Yamamoto. Improvement of pulmonary absorption of insulin and other water-soluble compounds by polyamines in rats. J. Control. Release 122 (2007) 94-101.

[38] Z. Dong, H. Katsumi, T. Sakane, A. Yamamoto, Effects of polyamidoamine (PAMAM) dendrimers on the nasal absorption of poorly absorbable drugs in rats. Int. J. Pharm. 393 (2010) 244-252.

[39] Y. Li, Y. Quan, L. Zang, M. Jin, F. Kamiyama, H. Katsumi, A. Yamamoto, S. Tsutsumi, Transdermal delivery of insulin using trypsin as a biochemical enhancer. Biol. Pharm.

Bull. 31 (2008) 1574-1579.

[40] M.E. Doyle, J.M. Egan, Mechanisms of action of glucagon-like peptide 1 in the pancreas. Pharmacol.Ther. 113 (2007) 546-593.

[41] B. Gallwitz, New therapeutic strategies for the treatment of type 2 diabetes mellitus based on incretins. Rev.Diabet. Stud. 2 (2005) 61-69.

[42] J.F. Todd, S.R. Bloom, Incretins and other peptides in the treatment of diabetes. Diabet. Med. 24 (2007) 223-232.

[43] D.J. Drucker, M.A. Nauck, The incretin system: glucagon-like peptide-1 receptor agonists and dipeptidyl peptidase-4 inhibitors in type 2 diabetes. Lancet 368 (2006) 1696-1705.

[44] D.G. Parkes, R. Pittner, C. Jodka, P. Smith, A. Young, Insulinotropic actions of exendin-4 and glucagon-like peptide-1 *in vivo* and *in vitro*. Metabolism 50 (2001) 583-589.

[45] O.G. Kolterman, B. Buse, M.S. Fineman, E. Gaines, S. Heintz, T.A. Bicsak, K. Taylor, D. Kim, M. Aispoma, Y. Wang, A.D. Baron, Synthetic exendin-4 (exenatide) significantly reduces postprandial and fasting plasma glucose in subjects with type 2 diabetes. J.Clin.Endocrinol.Metab. 88 (2003) 3082-3089.

[46] L.L. Nielsen, A.A. Young, D.G. Parkes, Pharmacology of exenatide (synthetic exendin-4): a potential therapeutic for improved glycemic control of type 2 diabetes. Regul.Pept. 117 (2004) 77-88.

[47] M. Szayna, M.E. Doyle, J.A. Betkey, H.W. Holloway, R.G. Spencer, N.H. Greiq, J.M. Egan, Exendin-4 decelerates food intake, weight gain, and fat deposition in Zucker rats. Endocrinology 141 (2000) 1936-1941.

[48] B. Zinman, B.J. Hoogwerf, S. DuránGarcía, D.R. Milton, J.M. Giaconia, D.D. Kim, M.E. Trautmann, R.G. Brodows, The effect of adding exenatide to a thiazolidinedione in suboptimally controlled type 2 diabetes: a randomized trial. Ann. Intern. Med. 146 (2007) 477-485.

[49] R.S. Cvetkovic, G.L. Plosker, Exenatide: a review of its use in patients with type 2 diabetes mellitus (as an adjunct to metformin and/or a sulfonylurea). Drugs 67 (2007) 935-954.

[50] C.S. Kolli, A.K. Banga, Characterization of solid maltose microneedles and their use for transdermal delivery. Pharm. Res. 25 (2008) 104–113.

[51] W. Martanto, J.S. Moore, T. Couse, M.R. Prausnitz., Mechanism of fluid infusion during microneedle insertion and retraction. J. Control. Release 112 (2006) 357-361.

[52] F.J. Verbaan, S.M. Bal, D.J. van den Berg, W.H. Groenink, H. Verpoorten, R. Lüttge, J.A. Bouwstra, Assembled microneedle arrays enhance the transport of compounds varying over a large range of molecular weight across human dermatomed skin. J. Control. Release 117 (2007) 238-245.

[53] K.V. Roskos, R.H. Guy, Assessment of skin barrier function using transepidermal water loss: effect of age. Pharm. Res. 6 (1989) 949-953.

[54] C. Rosado, P. Pinto, L.M. Rodrigues, Modeling TEWL-desorption curves: a new practical approach for the quantitative *in vivo* assessment of skin barrier. Exp. Dermatol. 14 (2005) 386-390.

[55] S.M. Bal, J. Caussin, S. Pavel, Joke A. Bouwstra, *In vivo* assessment of safety of microneedle arrays in human skin, Eur. J. Pharm. Sci. 35 (2008) 193-202.

[56] M. I. Haq, E. Smith, D. N. John, M. Kalavala, C. Edwards, A. Anstey, A. Morrissey, J. C. Birchall, Clinical administration of microneedles: skin puncture, pain and sensation, Biomed. Microdevices 11 (2009) 35-47.

[57] J.W. Fluhr, O. Kuss, T. Diepgen, S. Lazzerini, A. Pelosi, M. Gloor, E. Berardesca, Testing for irritation with a multifactorial approach: comparison of eight non-invasive measuring techniques on five different irritation types. Br. J. Dermatol 145 (2001) 696–703.

[58] M.M. Badran, J. Kuntsche, A. Fahr, Skin penetration enhancement by a microneedle device (Dermaroller®) *in vitro*: Dependency on needle size and applied formulation, Eur.

J. Pharm. Sci. 36 (2009) 511-523.

[59] D.J. Davies, R.J. Ward, J.R. Heylings, Multi-species assessment of electrical resistance as a skin integrity marker for *in vitro* percutaneous absorption studies. Toxicol. *InVitro*.18 (2004) 351–358.

[60] T.O. Herndon, S. Gonzalez, T.R. Gowrishankar, R.R. Anderson, J.C. Weaver, Transdermal microconduits by microscission for drug delivery. BMC Med. 2 (2004) 1-12.

[61] S.S. Lanke, C.S. Kolli, J.G. Strom, A.K. Banga, Enhanced transdermal delivery of low molecular weight heparin by barrier perturbation. Int. J. Pharm. 365 (2009) 26–33.

[62] T. Yamamoto, Y. Yamamoto, Electrical properties of the epidermal stratumcorneum. Med. Biol. Eng. (Mar.) (1976) 151–158.

[63] J.H. Draize, G. Woodard, H.O. Calvery, Methods for the study of irritation and toxicity of substances applied topically to the skin and mucous membranes. J. Pharmacol. Exp. Ther. 82 (1944) 377–390.

[64] X.H. Feng, R. Pelton, M. Leduc, Mechanical properties of polyelectrolyte complex films based on polyvinylamine and carboxymethyl cellulose, Indust. Engineer. Chem. Res., 45 (2006) 6665–6671.

[65] N. Roxhed, B. Samel, L. Nordquist, P. Griss, G. Stemme, Painless drug delivery through microneedle-based transdermal patches featuring active infusion. IEEE Trans. Biomed. Eng. 55 (2008) 1063–1071.

[66] P. Mikolajewska, R.F. Donnelly, M.J. Garland, D.I.J. Morrow, T.R.R. Singh, V. Iani, J. Moan, A. Juzeniene, Microneedle pre-treatment of human skin improves 5-aminolevulinic acid (ALA)- and 5-aminolevulinic acid methyl ester (MAL)-induced PpIX production for topical photodynamic therapy without increase in pain or erythema, Pharm. Res. 27 (2010) 2213-2220.

[67] Y. Wu, Y. Gao, G. Qin, S. Zhang, Y. Qiu, F. Li, B. Xu, Sustained release of insulin through skin by intradermal microdelivery system, Biomed. Microdevices 12 (2010)

665-671.

[68] L. Nordquist, N. Roxhed, P. Griss, G. Stemme, Novel microneedle patches for active insulin delivery are efficient in maintaining glycaemic control: An initial comparison with subcutaneous administration. Pharm. Res. 24 (2007) 1381-1388.

[69] W. Martanto, S.P. Davis, N.R. Holiday, J. Wang, H.S. Gill, M.R. Prausnitz, Transdermal delivery of insulin using microneedles*in vivo*. Pharm. Res. 21 (2004) 947-952.

[70] S.P. Sullivan, D.G. Koutsonanos, M. Del Pilar Martin, J.W. Lee, V. Zarnitsyn, S.O. Choi, N. Murthy, R.W. Compans, I. Skountzou, M.R. Prausnitz, Dissolving polymer microneedle patches for influenza vaccination. Nat. Med. 16 (2010) 915-20.

[71] M. Arakawa, C. Ebato, T. Mita, T. Hirose, R. Kawamori, Y. Fujitani, H. Watada, Effects of exendin-4 on glucose tolerance, insulin secretion, and beta-cell proliferation depend on treatment dose, treatment duration and meal contents. Biochem.Biophys. Res.Commun. 390 (2009) 809-814.

[72] T. Edholm, K. Cejvan, S.M. Abdel-Halim, S. Efendic, P.T. Schmidt, P.M. Hellstrom, The incretin hormones GIP and GLP-1 in diabetic rats: effects on insulin secretion and small bowel motility. Neurogastroenterol.Motil. 21 (2009) 313-321.

PUBLISHED PAPERS

1). Shu Liu, Mei-na Jin, Ying-shuQuan, Fumio Kamiyama, KosukeKusamori, Hidemasa Katsumi, ToshiyasuSakane, and Akira Yamamoto: Transdermal delivery of relatively high molecular weight drugs using novel self-dissolving microneedle arrays fabricated from hyaluronic acid and their characteristics and safety after application to the skin. *European Journal of Pharmaceutics and Biopharmaceutics*, **86**, 267-276 (2014). [Chapter 1]

2). Shu Liu, Mei-na Jin, Ying-shuQuan, Fumio Kamiyama, Hidemasa Katsumi, ToshiyasuSakane, and Akira Yamamoto: The development and characteristics of novel microneedle arrays fabricated fromhyaluronic acid, and their application in the transdermal delivery of insulin. *Journal of Controlled Release*, **161**,933－941 (2012). [Chapter 2]